ORIENTATIONS OF DIPOLE ANTENNA FOR DOUBLE STACKING HYDROCARBON MARINE CONTROLLED SOURCE ELECTROMAGNETIC

by

NORHANIS BINTI NAHAR (11403)

Dissertation submitted in partial fulfilment of

the requirements for the

Bachelor of Engineering (Hons)

(Electrical Electronic Engineering)

Supervised by Prof Dr. Noorhana Yahya

MAY 2012

Universiti Teknologi PETRONAS

Bandar Seri Iskandar

31750 Tronoh

Perak Darul Ridzuan

ORIENTATIONS OF DIPOLE ANTENNA FOR DOUBLE STACKING HYDROCARBON MARINE CONTROLLED SOURCE ELECTROMAGNETIC

by

Norhanis Binti Nahar

A project dissertation submitted to the
Electrical & Electronics Engineering Programme
Universiti Teknologi PETRONAS
in partial fulfilment of the requirement for the
Bachelor of Engineering (Hons)
(Electrical & Electronics Engineering)

Approved:

____

Prof. Dr. Noorhana Yahya
Project Supervisor

UNIVERSITI TEKNOLOGI PETRONAS
TRONOH, PERAK

May 2012

CERTIFICATION OF ORIGINALITY

This is to certify that I am responsible for the work submitted in this project, that the original work is my own except as specified in the references and acknowledgements, and that the original work contained herein have not been undertaken or done by unspecified sources or persons.

(Norhanis bt Nahar)

ACKNOWLEDGEMENTS

This final year project would not have been possible without the guidance and the help of several individuals who in one way or another contributed and extended their valuable assistance in the preparation and completion of this study.

First and foremost, praise to Allah the Almighty, who has helped and gave me courage and strength in completing Final Year Project (FYP). Without His permission, this FYP will not be a success.

My utmost gratitude to my supervisor Prof. Dr. Noorhana Yahya for the continuous support of my final year project, for her patience, motivation, enthusiasm, and immense knowledge. Her guidance helped me in all the time of research and writing of this final report. I could not have imagined having a better supervisor and mentor for my final year project.

Besides my supervisor, I would like to thank both Dr. Afza Shafie', Pn. Hanita and also Mr. Kashif for his assistance on how to use the software needed for my project. Engineering student who in one way or another were helps in giving assistance to understand the physics part of my project.

I would like to thank my family: especially my parents Nahar b. Md Nor and Khadijah bt. Said, for and supporting me spiritually throughout my life, they are my key sources of strength in whatever I do in my life. Thank you so much for always be there through my ups and downs.

I would like to take this opportunity to express my deepest gratitude to all parties involved in conducting this project ranging from UTP lecturers, and my friends especially Nik Nur Shahirah, Iryani and Sakinah who have been supportive in helping me doing the project. Last but not least, many thanks to others whose name was not mentioned in this page but has in one way or another contributed to the accomplishment of this project.

TABLE OF CONTENTS

LIST OF TABLES

LIST OF FIGURES

ABSTRACT

Seabed logging is an innovative electromagnetic (EM) method of locating offshore hydrocarbon reservoir. It is a technique that utilizes Electromagnetic (EM) waves to propagate signals to reservoir depths where the difference in resistivity levels of different regions under the seafloor will help to determine possible oil wells for future exploration. However, different antenna orientation varies the sensitivity in detecting hydrocarbon layer. The correct rotation and placement of antenna will give the best response in optimizing the accuracy of oil layer position in seabed. In addition, it is very difficult to predict the existing 2^{nd} hydrocarbon underneath the sea. Thickness oil layer variation will vary the magnitude of field received by the receiver. In this project, 2D modeling will be constructed by using CST EM Studio as simulator software. At the end of this project, the simulator could show the sensitivity of of each antenna orientation and responses from the two oil layers. From simulations, Horizontal Electric Dipole, in-line with receiver (HED-R), is the most sensitive in detecting one hydrocarbon layer with 380% increased in magnitude of E-field compared to Vertical Electric Dipole (VED) . The magnitude of E-field increase when the oil layer thickness increased and viceversa. For every 50m increment of oil layer thickness, 20% of the E-field magnitude will be increased. E-field magnitude deviated to the decrease of 46% when the 2^{nd} hydrocarbon layer been decreased to 30m. The minimum percentage of starting point of hydrocarbon to be considered is 1% and the highest percentage field difference is taken as the ending point of hydrocarbon. The percentage of E field increased as minimum as 1% after 3000m the original location of hydrocarbon. In conclusion, Vertical Electric Dipole antenna gives the most optimum senstivity in detecting stacking of hydrocarbon layer with the highest percentange difference increment of 11.21% compared to both Horizontal Electric Dipole (HED) antennas. This report will also describe briefly on the advantages of this technique as well as the process involved on the project.

CHAPTER 1

INTRODUCTION

1.1 Background of Study

A special application of frequency domain that uses controlled-source electromagnetic (CSEM) method, seabed logging, measures the electrical resistivity beneath the seafloor in hydrocarbon exploration, reservoir assessment and development. The simple basic principle which makes a potential tool in the offshore exploration is based on the electrical resistivity contrast between a hydrocarbon bearing reservoir and surrounding host rocks. The reason for this is also based on the fact the water supports free ions and easily transports electric current whereas oil acts as an insulator.

With different antenna configurations, the transmitted electromagnetic wave enters the high resistive hydrocarbon layer under a critical layer and is guided along the layer. Then, the signal leak form the layer and reflected back to the receiver at the seafloor. Seabed logging method records the presence of electrically resistive bodies in the earth, descriminating between water-saturated sea rock and hydrocarbon.

Various techniques including the study of seismic analysis and landforms are essential for obtaining accurate sub-seafloor resistivity data. Using the latest controlled source electromagnetic technology, several data regards to the types and orientations of the dipole antenna can be gathered, the thickness of the layer can be varies accurately determined the responses, in finding trapped hydrocarbon in the subsurface prior to drilling.

1.2 Problem Statement

The problem statements of this project are:

i. Different antenna orientation varies the sensitivity to detect hydrocarbon layer in seabed logging.

ii. It is very difficult to predict the existing 2^{nd} layer hydrocarbon underneath the sea floor. Modeling of SBL for simulation under deep water environment using suitable electromagnetic modeling technique to differentiate between water, sediment and hydrocarbon layer are needed.

1.3 Objectives

The objectives of this project are:

i. To investigate the best antenna orientations that are sensitive in detecting double hydrocarbon layer.

ii. To determine the effect and response of field received (E-field) magnitude when the thickness and position of the upper layer hydrocarbon are varied.

iii. To observe the airwave effects on the two layers hydrocarbon in Magnitude vs Offset (MVO) graph.

1.4 Scope of Study

In order to complete this project, several scope of study had to achieve. The major scopes are as follows:

1.4.1 Understanding Seabed Logging method.

- The modeling of SBL simulation required a firm knowledge and research towards seabed logging technique and the idea on how the process involved, current existing issue to get better clarification.
- Research on electromagnetic theory and wave and also the measurement principle of seabed logging to transmit EM waves beneath the sea floor.
- The data handling of receivers.

1.4.2 Developing Seabed Logging modeling using CST EM Studio

- CST EM Studio will be needed to install inside author's personal computer.
- There will be a research and training on how to use the CST EM Studio in order to develop the simulator.
- The result simulator will be used in determined the sensitivity of the source/receiver combination in seabed logging method.

1.5 Feasibility of Project

For the first semester, the author will start with research development on the basic principle of electromagnetic waves, and its application of the simulator. It includes SBL operations, techniques, advantages and disadvantages, the issues related for the future cases in SBL.

With the resources provided by the University, the project can be completed within the given time.

CHAPTER 2

LITERATURE REVIEW

2.1 Seismic Method

Hydrocarbon exploration using seismic method has become the most accurate and frequently used because it can detect potential hydrocarbon reservoir beneath the seafloor. It maps the boundary layers based on different acoustic properties [2].

According to [2], acoustic waves are used to map boundaries between layers with contrasting acoustic properties. A sound source that is attached to the ship sends sound waves through the water. As the sound waves are release, the rock layers beneath the seafloor reflect this sound. Using seismic method, the presences of water or hydrocarbon in the traps can not be differentiated [2]. Depending on seismic data, the success rate of commercially viable exploration wells, is about 10-30% [5]

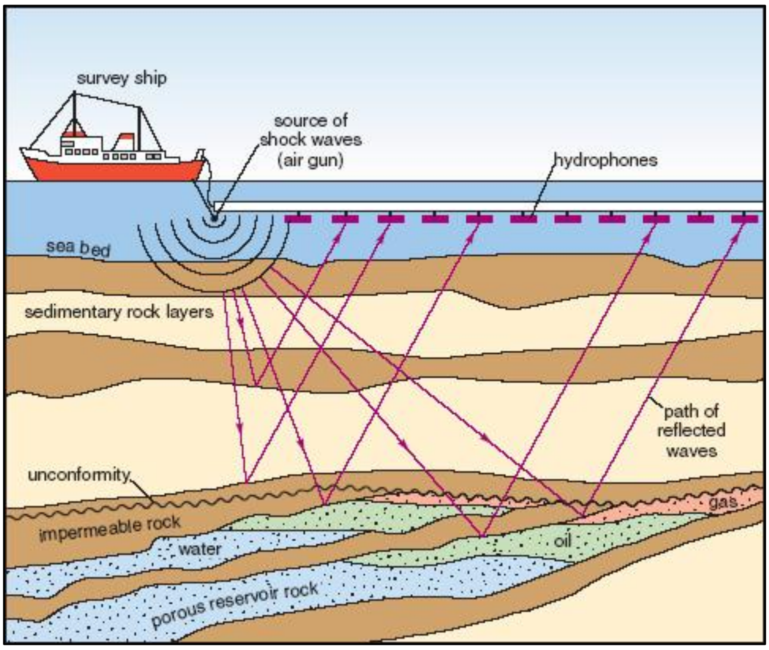

Figure 1: Illustration of seismic reflection profiling [1]

2.2 Controlled Source Electromagnetic (CSEM)

By using controlled source electromagnetic (CSEM) method, it can effectively differentiate between different types of offshore reservoir fluids as fluids like oil and gas are typically characterized by a lower electrical conductivity than brines and water. This method measures electromagnetic fields sensors on the ocean floor. A deep-towed transmitting antenna then generates low-frequency electromagnetic fields, which are detected by the sensor. Both antenna tow lines and sensor arrays can cover areas ranging to thousands of square kilometers [6].

2.3 Seabed Logging

Seabed Logging (SBL) is an application of the marine controlled source electromagnetic (CSEM) method that is used to directly detect and characterize possible hydrocarbon-bearing prospects [3]. This technique uses electromagnetic waves that are able to distinguish the two liquids (water and hydrocarbon) based on their large differences in resistivity values. Hydrocarbon reservoirs are known to have resistivity value of 30-500 Ωm in contrast to sea water of layer of 0.5 – 2 Ωm and sediments of 1 – 2 Ωm. The reason for this is based on the fact that water supports free ions and easily transports electric current whereas oil acts as an insulator [4].

SBL uses a mobile horizontal electric dipole (HED) source that is towed by a vessel at about 30m above an array of seafloor electric field receivers. This HED is emitting a low frequency (typically 0.1 to 10Hz), continuous electromagnetic signal into seawater and down into the subsurface and in upwards directions to the water-air interface [4]. Each electrode is electrically connected to a signal generator, transmitting a continuous periodic signal with any curve shape and frequency ranging from 0.05Hz to 10Hz. A maximum current of 1250A are applied and peak-to-peak current are kept constant. The distance from the source to the seabed is monitored by an echo sounder [8].

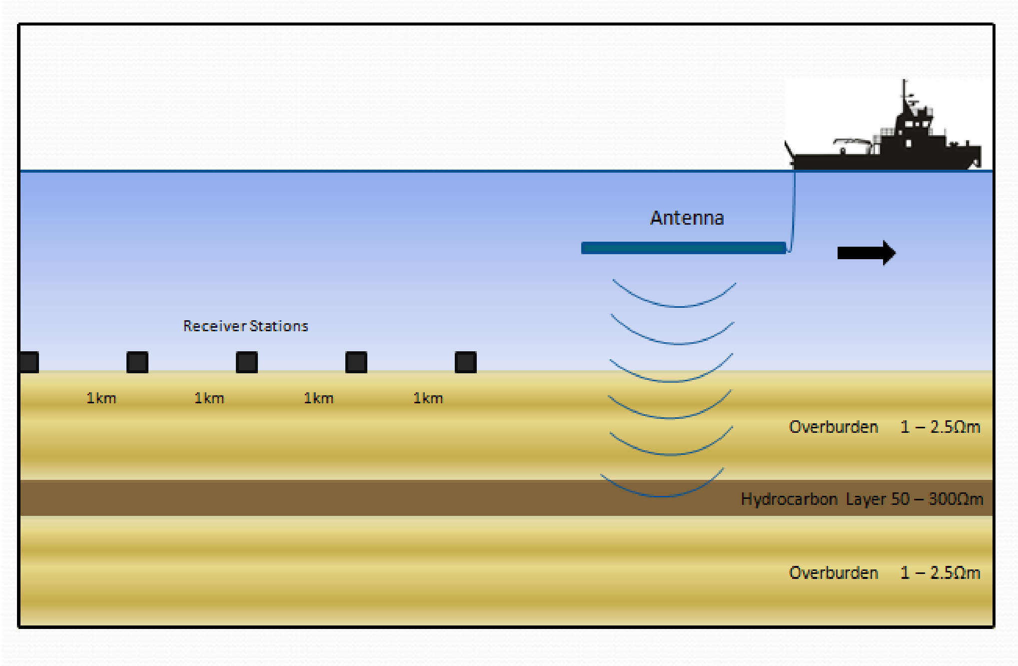

Figure 2: Seabed logging process

The receiver are dropped from the survey vessel and sinks freely down to the seabed. The exact receiver position is determine by acoustic ultra short baseline communication. A concrete anchor held the receiver in position at the seabed. After the recording period, an acoustic signal from the vessel triggers a release mechanism, causing the receiver to release from their anchors and float back to the surface. The receiver consist of a buoyancy system (5 yellow spheres at the top of the receiver), a data acquisition unit (white cubic box), an anchor, and sensors (two pairs of orthogonal electric sensor and two pairs of magnetic sensor). The receiver record the electric and magnetic field as time series before they are processed into the frequency domain and combined with navigation data [8]. The receiver also record the transmitted signal in the form of direct waves, air waves reflected waves and guided waves [4]. Seabed logging delivers subsurface resistivity information before drilling a well. Although the resolution is lower than from borehole logging or seismic imaging, the technique is an excellent ‘edge detector’ and greatly improves reservoir delinenation.

2.4 EM Transmitter

The electromagnetic waves transmitted from the EM transmitter diffuse in all direction. The receivers placed on the sea floor captures three kinds of waves. First is direct wave directly to the sea floor detectors from the transmitter. Second is the air wave which is reflected and refracted through water air interface. The third is the guided wave, the only reflected and refracted from high resistive layers under the seabed. The electromagnetic waves which are refracted back from the high resistive subsurface layers predict about the hydrocarbon. The high resistive layer cannot be predicted if the target is deeper at particular frequency. [9]

2.5 Air Waves

In shallow-water (500m-1000m) hydrocarbon exploration, the air layer creates a problem: the source-induced airwave component. The airwave component is predominantly generated by the signal component that diffuses vertically upward due to small angle from the vertical at seafloor, will occur total reflection occurs from the source to the sea surface, the wave then propagates through the air at the speed of light without attenuation through the water layer before diffusing back down vertically to the sea bottom, recorded by the receiver on the seafloor. Even though a diffusion field is measured, the field is called the airwave, where it is picked up instantly. Because of nearly instant propagation, the airwave can be treated as a potential field in the atmosphere. [19]

2.6 Stacking Layer

Hydrocarbon entrapment takes place when the rocks defining the bounding surfaces of a valid trapping geometry possess hydrocarbon sealing properties. The hydrocarbons are buoyant and have to be trapped within a structural. Two or more hydrocarbon layer underneath seafloor are mainly be focused on to maximize profit and to reduce exploration costs.

2.7 Theory

This section discussion on the basic theories involve in conducting data processing in SBL.

2.7.1 Wave Propagation Paths in a Hydrocarbon Reservoir

In seabed logging, the energy of electromagnetic waves is guided along the oil layers and attenuated to a certain extent. In high resistance layers such as hydrocarbon, skin depth in the seabed are longer and at a critical angle of incidence, energy refracted back to the seabed and detected by electromagnetic receivers positioned thereupon [9] The received data is processed and presented in two dimensional model to map the oil layer. There are five component of received EM waves which are:

i. Air waves : EM waves reflected back at the boundary of air and seawater.
ii. Direct waves : EM waves from transmitter
iii. Reflected waves : EM waves from the seabed or host rock
iv. Reflected waves : EM waves from hydrocarbon
v. Guided waves : EM waves through hydrocarbon

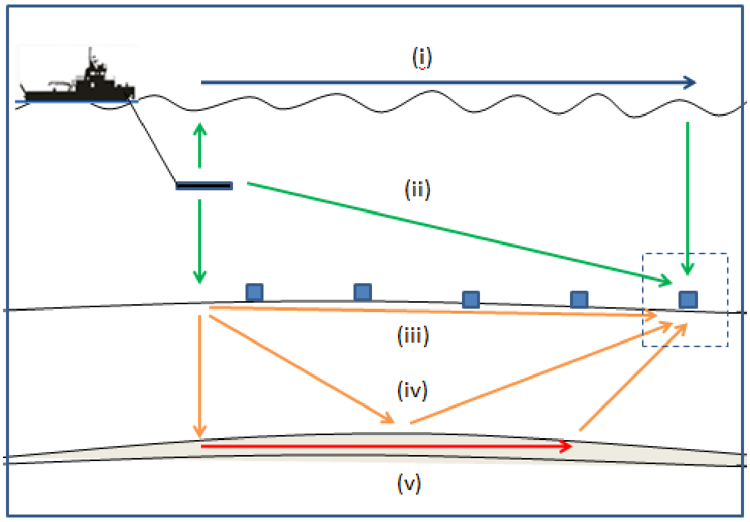

Figure 3 : Schematic Diagram of EM Waves in the form of Air Waves, Direct Waves, Reflected Waves and Guided Waves [20]

In figure, a combination of energy pathways including signal transmission directly through seawater, reflection and refraction via the seawater-air interface, refraction and reflection along the seabed, and reflection and refraction via possible high resistivity subsurface layers are recorded by the seabed receivers.

Low frequency EM waves decay exponentially with distance z (m) by $e^{-z/\delta}$ where:

$$\boldsymbol{\delta} = \sqrt{\frac{\mathbf{2}\boldsymbol{\rho}}{(\mathbf{8} \times \mathbf{10^{-7}})(\boldsymbol{\pi^2})(\boldsymbol{f})}} \quad (1)$$

Where

ρ = resistivity (Ωm)

f = signal frequency (Hz)

The distance required to attenuate an EM signal by the factor $e^{-1}(0.37)$ is defined as the skin depth and is about 780 m in seawater (0.3 Ωm), 2013 m in 2 Ωm sediment and $4E^8$ m in air (10^{10}Ωm) for a 0.125 Hz signal. EM signals are rapidly attenuated in seawater and seafloor sediments saturated with saline water, and these signal pathways will dominate at near source-to-receiver offsets (~ 3 km)

2.7.2 Wave Equation

Propagation constant, γ is defined as,

$\gamma = \alpha + j\beta$,

where,

$$\boldsymbol{\alpha} = \boldsymbol{\omega}\sqrt{\mu\boldsymbol{\omega}}\left[\frac{\mathbf{1}}{\mathbf{2}}\left(\sqrt{\mathbf{1} + \left(\frac{\boldsymbol{\sigma}}{\boldsymbol{\omega\varepsilon}}\right)^2} - \mathbf{1}\right)\right]^{\frac{1}{2}}$$

$$\boldsymbol{\beta} = \boldsymbol{\omega}\sqrt{\mu\boldsymbol{\omega}}\left[\frac{\mathbf{1}}{\mathbf{2}}\left(\sqrt{\mathbf{1} + \left(\frac{\boldsymbol{\sigma}}{\boldsymbol{\omega\varepsilon}}\right)^2} + \mathbf{1}\right)\right]^{\frac{1}{2}}$$

For magnitude of received wave,

$$\mathbf{E_x} = \boldsymbol{E}\boldsymbol{e}^{(-\alpha z)}\boldsymbol{e}^{(-j\beta z)}$$

To calculate intrinsic impedance, η of the medium,

$$\boldsymbol{\eta} = \sqrt{\frac{\boldsymbol{j\omega\mu}}{\boldsymbol{\sigma + j\omega\varepsilon}}}$$

The parameter α is commonly called as attenuation constant which will provide the amplitude of decay, and β is called phase constant, which provide phase propagation for the wave. By some approximate relations:

If $\sigma >> \omega\varepsilon$

This indicates that in such cases,

$$\boldsymbol{\alpha = \beta \approx \sqrt{\frac{\omega\mu\sigma}{2}} = \frac{1}{\delta}}$$

where δ is the skin depth.

2.7.3 Fundamental of Fields and Waves

Modern electromagnetism formulas are being used in the project. It is based on a set of four fundamental relations known as Maxwell's equations. Together with some auxiliary relations, Maxwell's equations form fundamental tenets of electromagnetic theory.

$$\nabla \bullet \mathbf{D} = \rho_v$$

$$\nabla \times \mathbf{E} = \frac{\partial \boldsymbol{B}}{\partial \boldsymbol{t}}$$

$$\nabla \bullet \mathbf{B} = 0$$

$$\nabla \times \mathbf{H} = \mathbf{J} + \frac{\partial \boldsymbol{D}}{\partial \boldsymbol{t}}$$

where:

$\mathbf{D} = \varepsilon\mathbf{E}$

$\mathbf{B} = \mu\mathbf{H}$

$\mathbf{J} = \sigma\mathbf{E}$

$\varepsilon = \varepsilon_0 * \varepsilon_r$

$\mu = \mu_0 * \mu_r$

2.6.3.1 Gauss Law

In quantitative approach of Gauss Law, the mathematical formula for electric flux must include the effect of angle between surface and the field lines.

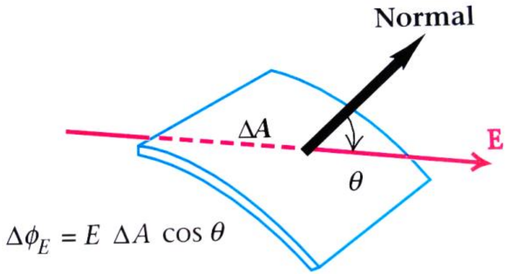

Figure 4 : Electric field passing through a small surface of area A.

The normal to the surface makes an angle θ with the direction of the electric field . The electric flux is equal to the product of the field strength E, the area A, and the cosine of the angle between the direction of the field and the surface normal [21]

2.7.4 Electromagnetic Waves

In electromagnetic waves most of the theory is related to Maxwell's equations and it is stated that magnetic field produced (B) is proportionally related to the current and the type of material used. The bigger the current flows inside a conductor and the higher the permeability of the material used, then the bigger the B field is produced [9]. Both magnetic field (B) and electric field (E) are propagating perpendicularly to each other with the same amplitude where the reduction in B field intensity will cause the same amount of reduction in E field as well [9].

Based on Maxwell equation [9]:

$$\boldsymbol{B = \frac{\mu_0 I}{2\pi r}}$$

Where;

B = Magnetic field,	I = Current
μ_0 = Permeability	r= Distance

2.8 Experiment Parameters

Modeling

Features	Characteristic/Attributes/Units
Size • Length • Width	40000m^2 20000m 20000m
Layers	**Thickness**
• **Air** ▪ Thickness ▪ Material Set ▪ Type ▪ Epsilon ▪ Mue ▪ Electric conductivity	 500m Default Normal 1 1 1e-011 [S/m]
• **Seawater** ▪ Thickness ▪ Material Set ▪ Type ▪ Epsilon ▪ Mue ▪ Electric conductivity ▪ Thermal conductivity	 2000m Default Normal 81 0.999991 3.33 [S/m] 0.6 [W/K/m]
• **Sediment** ▪ Thickness ▪ Material Set ▪ Type ▪ Epsilon ▪ Mue ▪ Electric conductivity ▪ Thermal conductivity	 3200m Default Normal 30 1 0.5 [S/m] 0.65 [W/K/m]
• **Oil** ▪ Separation between oil ▪ Material Set ▪ Type ▪ Epsilon ▪ Mue ▪ Electric conductivity ▪ Thermal conductivity	 1000m Default Normal 4 1 0.004 [S/m] 0.15 [W/K/m]

Table 1: Modelling Parameters

CHAPTER 3

METHODOLOGY

3.1 Project Work

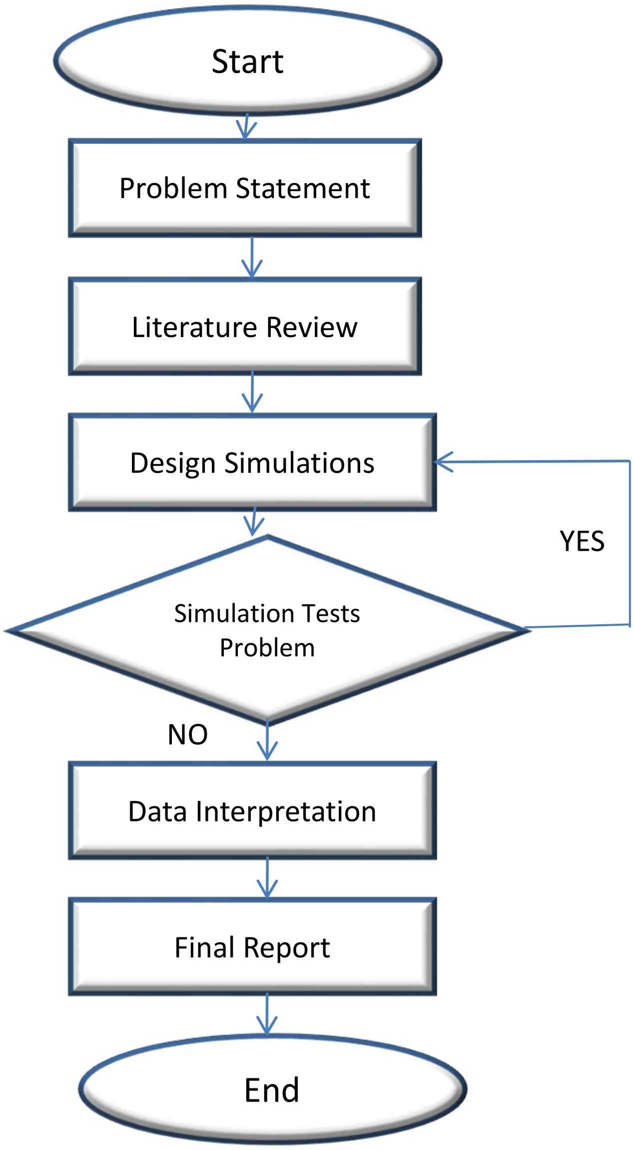

Figure 5: Flow Diagram for Project Work

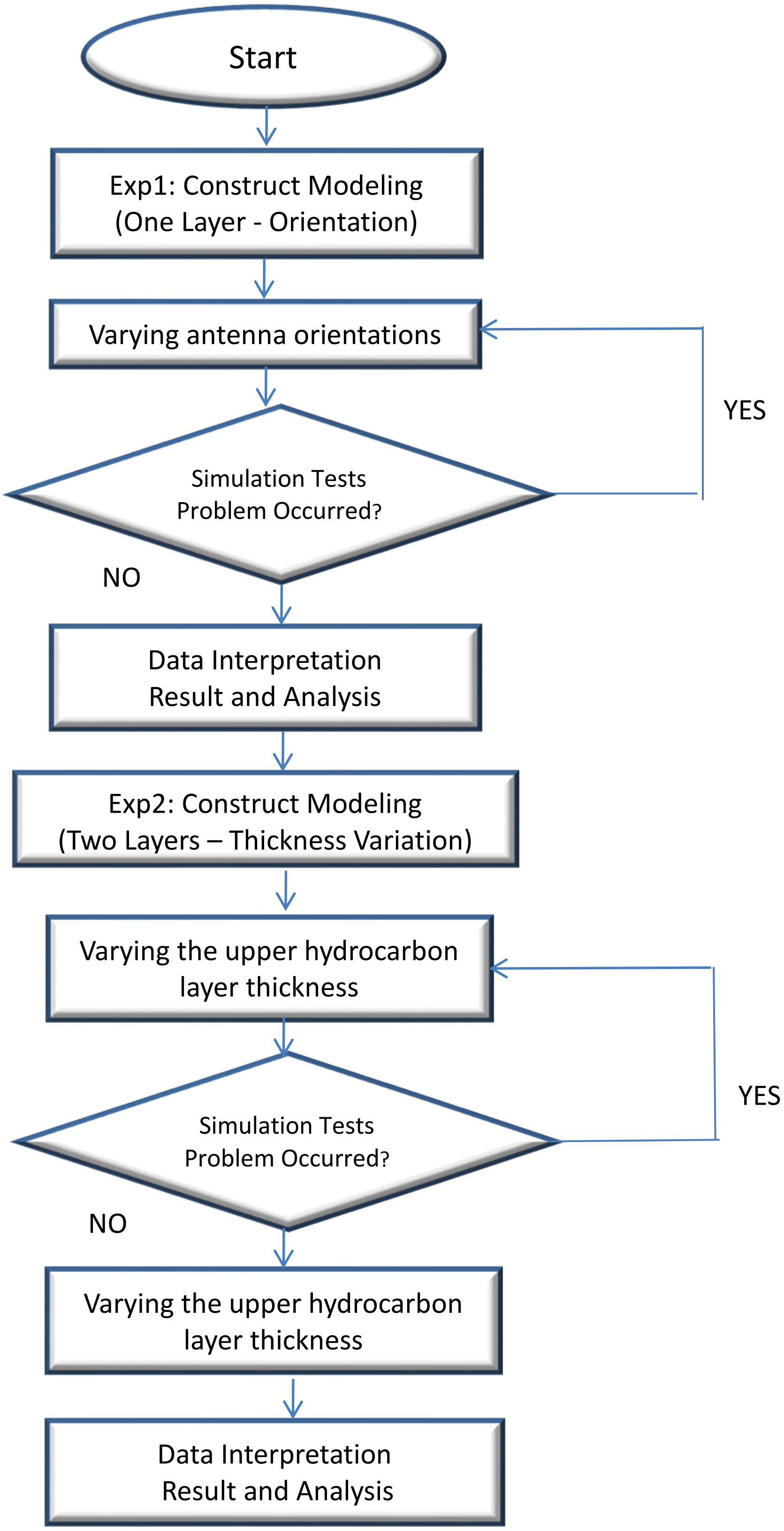

Figure 6 : Work Diagram of FYP1 Simulations

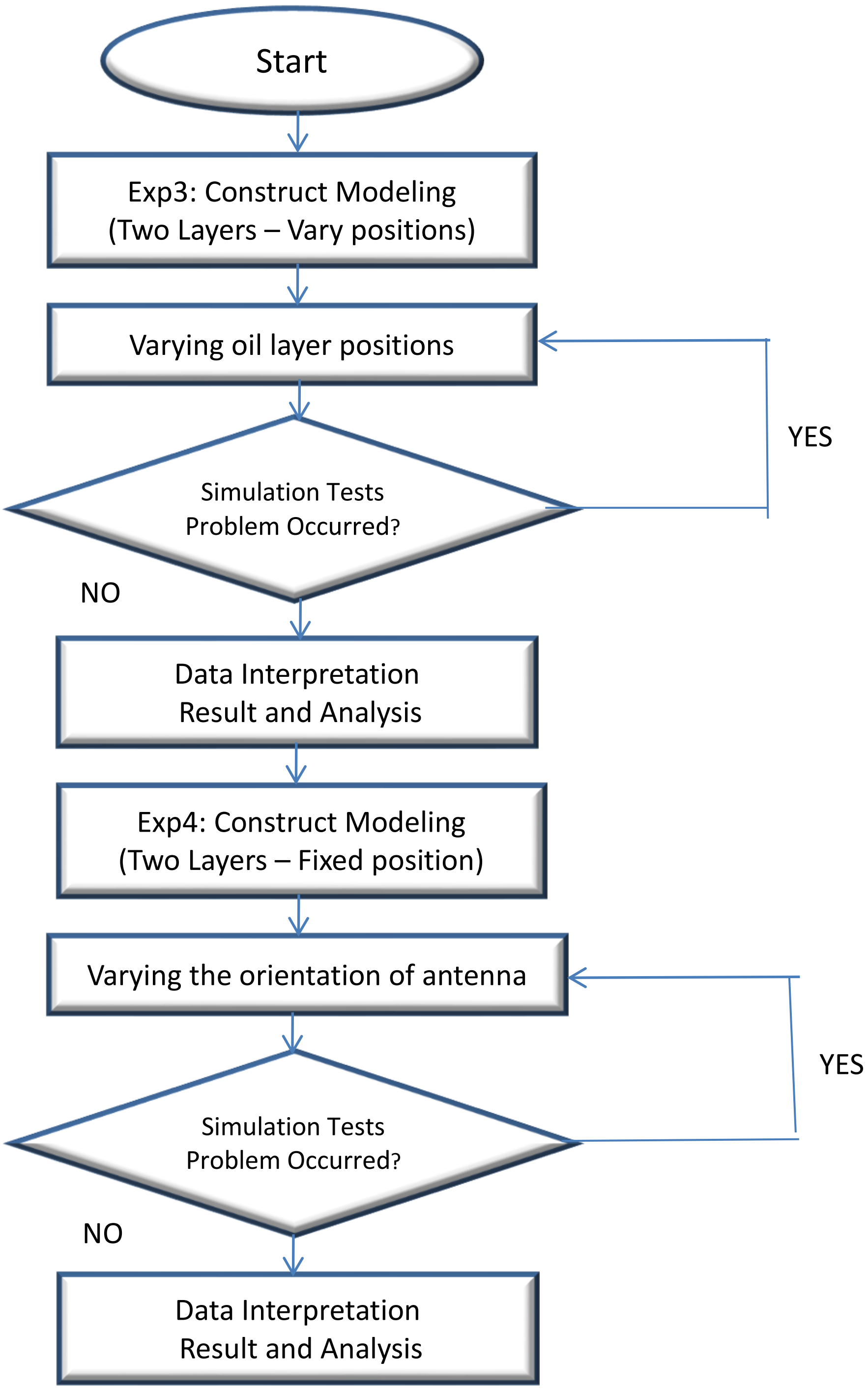

Figure 7 : Work Diagram for FYP2 Simulations

Implementation

The project is a simulation base project. Specifically, it is a comparison of antenna orientations and variation of hydrocarbon layer thickness and positions for detecting hydrocarbon layers in seabed logging (SBL). The project will begin with identification of problem statements on several issues related to SBL transmitter and receiver combinations in deep water condition.

For this project, the most important task is data gathering and research to acquire the theoretical equation, basic fundamental of antennas, the working principle, and some ideas design for model development. Journal, articles, papers, books from all sources regarding SBL and EM wave characteristics is essential to be referred and to ensure the accuracy of collected data. Since different orientations of transmitter and variation of layer thickness are being used for this project, a firm knowledge of designing and concept of antennas and modeling must be obtained to get the accurate result.

The next step is designing simulation by using CST EM STUDIO. As this is the most crucial part of the project, some techniques in developing forward modeling have to be learnt and the author must be able to simulate all antenna orientations in order to find the most sensitive combination in detecting oil layers. The received data in electric field will be processed as part of data representation in one dimensional view.

Lastly, all the studies and discussions will be compiled in the final report. The justification of the best combination of transmitter and receiver will be further explained from the study.

3.2 Research Methodology

In gaining information relating to the major scope of the project, various research have to be done. The research covers wide topic, especially on seabed logging technique and modeling from different source; e-journal, e-thesis, several trusted links, book, and papers.

The step of research:

- Information obtained in type and orientation of EM wave, their characteristic in different frequency. Propagation of wave inside water.
- The classification of parameters in deep water condition, which focus on vertical or horizontal, electric dipole combinations
- Layer thickness that affects the electric field (E-field) magnitude.
- Steps and techniques in 2D/3D modeling using CST EM Studio.
- Justification of obtained result.

3.3 Tool Required

i. **CST EM Studio**

Simulator software dedicated to the simulation of static and low frequency devices. It features a variety of solver module to tackle electrostatic, magneto statics, current flow, low frequency, and even stationary temperature problems. This software will be the main tool for developing the simulation of electromagnetic waves in seabed logging applications. Conventional models can be easily extended for one type of physics into multiphysics models that solve physics phenomena and do so simultaneously. By using this software, it enables the author to characterize, modeling design and varying the antenna orientations, improving overall performance.

3.3 Activities/Gantt Chart and Milestone

No	Detail/Week	1	2	3	4	5	6	Mid-Semester Break	7	8	9	10	11	12	13	14
1	Selection of Project Topic: Types and Orientation of Antenna for Hydrocarbon Detection (Two Layers) in Seabed Logging	■	■													
2	Preliminary Research Work: Research on literatures related to the topic		■	■	■	■										
3	Submission of Extended Proposal						■									
4	Project Work: Study on the research scope and method						■									
5	Viva: Proposal Defense and Progress Evaluation										■					
8	Project work continues: Further investigation on the project and do modification if necessary								■	■	■	■	■	■	■	■
9	Submission of Final Draft Interim Report														■	
10	Submission of Final Interim Report															■

Table 2: Gantt chart and Key Milestone for Final Year Project 1

No	Detail/Week	1	2	3	4	5	6	Mid Semester Break	7	8	9	10	11	12	13	14	15
1	Project Development: Types and Orientation of Antenna for Hydrocarbon Detection (Two Layers) in Seabed Logging																
2	Progress Report																
3	Pre-EDX																
4	Project Development:																
8	Submission of Final Draft Report																
9	Submission of Final Report																
10	Final Viva																

Table 3: Gantt chart and Key Milestone for Final Year Project 2

CHAPTER 4

RESULT AND DISCUSSIONS

This chapter describes the type and orientations of antennas between Horizontal Electric Dipole antenna in line with receiver (HED-R), Horizontal Electric Dipole antenna crossline with receiver (HED-P) and Vertical Electric Dipole antenna (VED) for deep water target hydrocarbon exploration. The modeling structures have been developed by using CST EM Studio that reflect the seabed logging 3D simulation. The simulator has been modified to observe the results by changing the orientation of the antenna, varying the hydrocarbon thickness and observing the response of fixed postion by ploting magnitude versus offset for different target depth were done. Table 1 and Table 2 shows the parameter setting for antenna and receiver used for the four experiments.

<u>Antenna</u>

Features	Characteristic/Attributes/Units
Shape	Cylindrical 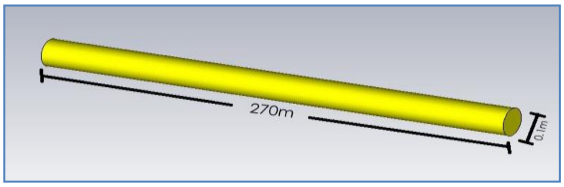
Material • Material Set • Type • Epsilon • Mue • Electric conductivity • Thermal conductivity • Heat capacity • Material density info	Aluminium Low Frequency Normal 1 1 3.72e+007 [S/m] 237.0 W/ (K m) 0 kJ / K / kg 0.0 kg / m^3

Length	270m
Diameter	0.1m
Radius • Outer radius • Inner Radius	 0.05m 0m
Orientation	Varied
Height from seabed	30m
Current Line	1250A

Table 4 : Antenna parameter

The simulation was done on a full scale. Aluminium and copper are commonly used for dipole antenna however for this project, aluminium is chosen due to its light weight, less corrosive and lower than copper.

Receiver

Features	Characteristic/Attributes/Units
Orientation	X axis
Length	40000m
Separation between receiver	1000m

Table 5 : Receiver parameters

4.1.1 Experiment 1: Varying the orientation of the antenna

The model that has a hydrocarbon layer has been developed to right side of the model (0-20000 m) in CST software. The size of model is 40000 m^2. The receiver is from offset of -20000 m to 20000 m detecting the response of electric field. The parameters are shown in the Figure 2 and Table 3 below. The antenna is been placed in 3 different orientation shown in Figure 10, 11, and 12. In this experiment, the author would like to determine the best antenna orientation for one layer hydrocarbon detection. The model used for this experiment is shown in Figure 8

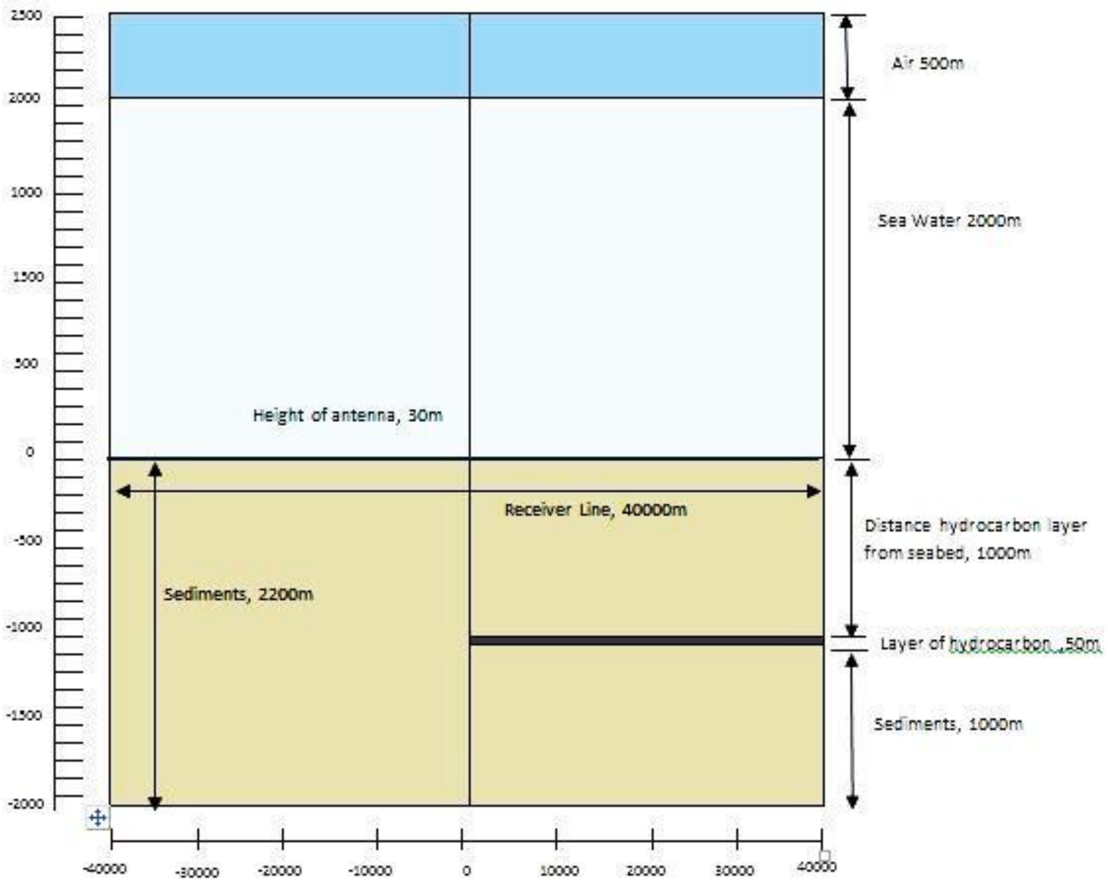

Figure 8 : Layer parameters for experiment 1

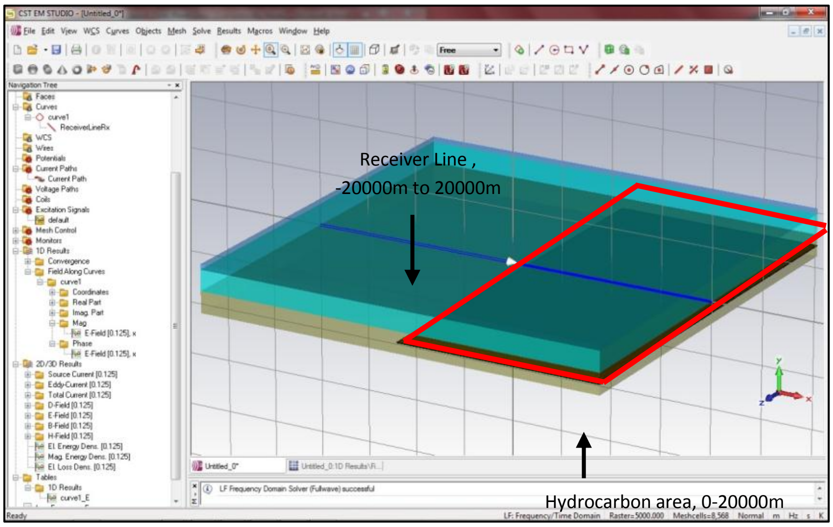

Figure 9 : 3D Modeling in CST software

Setting	Sea water	Hydrocarbon	Air	Sediment
Relative Permitivity	81	4	1	30
Electric Conductivity	3.33	0.004	1E-011	0.5

Table 6 : Parameter setting

Hexahedral mashes with electric boundary condition and a low frequency solver used to simulate the antenna. The dipole antenna with the length of 270 m and 1250A current are the two parameters being fixed. The antenna is placed with different orientations as shown in Figure 3-5 below. The receiver is fixed on x-direction.

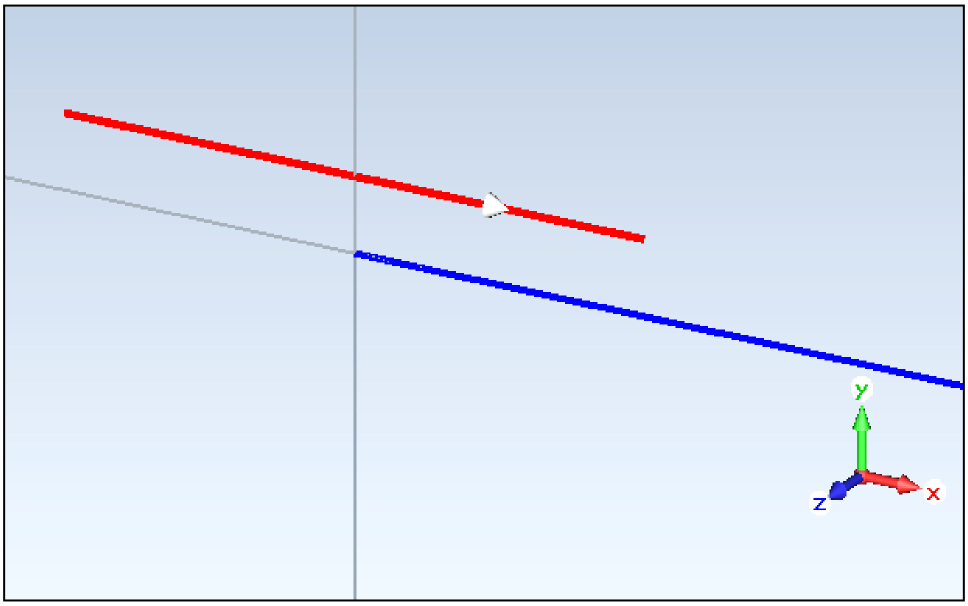

Figure 10 : Horizontal Electric Dipole Antenna,
inline with receiver (HED-R) – x direction

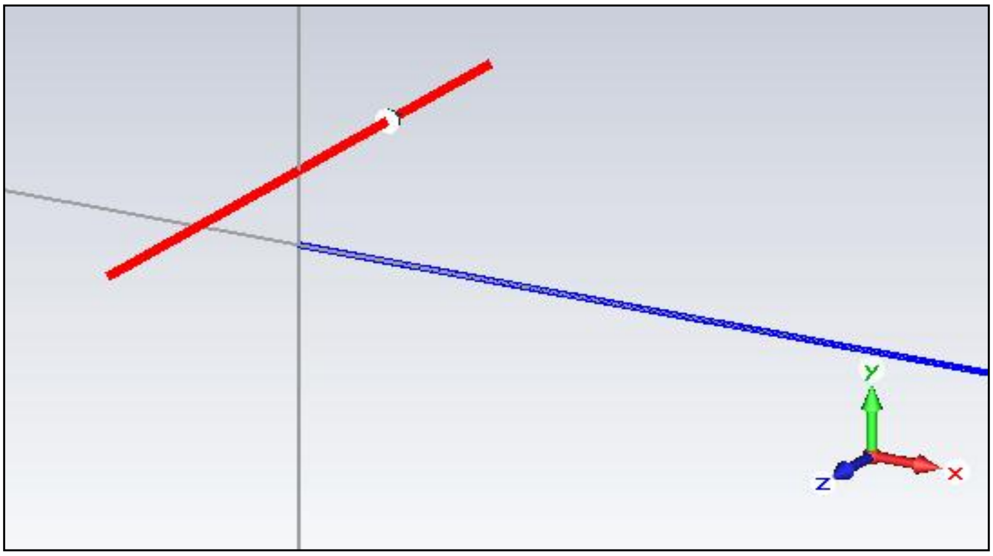

Figure 11 : Horizontal Electric Dipole Antenna,
crossline with receiver (HED-P) – z direction

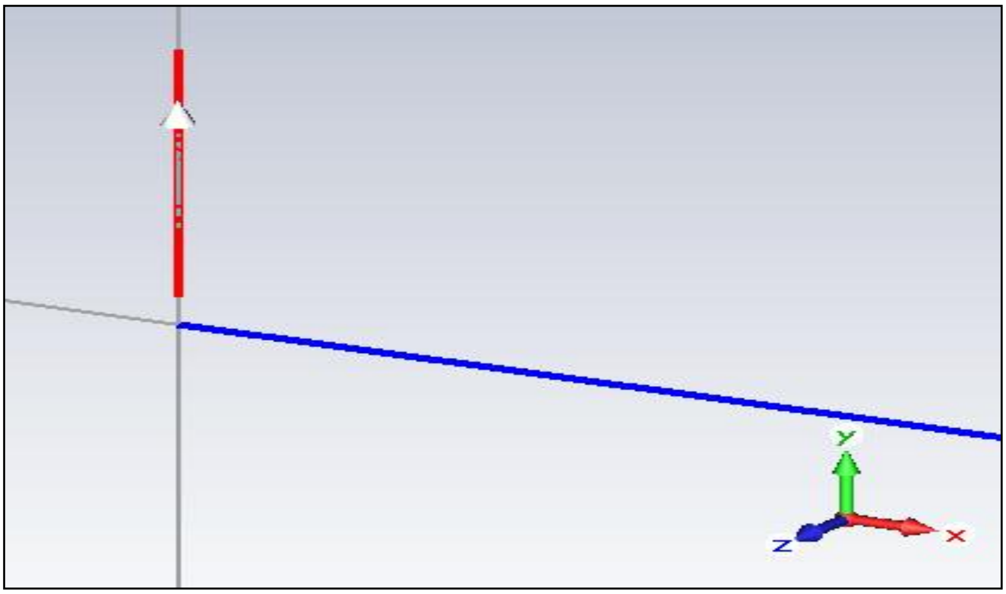

Figure 12: Vertical Electric Dipole Antenna (VED) – y direction

Results

Offset (m)	Inline E-Field [0.125], x/real	Crossline E-Field [0.125], x/real	Vertical E-Field [0.125], x/real	Offset (m)	Inline E-Field [0.125], x/real	Crossline E-Field [0.125], x/real	Vertical E-Field [0.125], x/real
0	1.19E-09	0	8.99E-12				
1000	1.19E-09	0	8.99E-12	**21000**	2.77E-05	0	6.95E-05
2000	1.21E-09	0	1.44E-11	**22000**	5.05E-06	0	1.31E-06
3000	1.22E-09	0	2.54E-11	**23000**	1.31E-06	0	1.69E-07
4000	1.26E-09	0	4.63E-11	**24000**	5.34E-07	0	1.15E-07
5000	1.35E-09	0	8.49E-11	**25000**	2.70E-07	0	7.37E-08
6000	1.59E-09	0	1.55E-10	**26000**	1.59E-07	0	4.71E-08
7000	2.07E-09	0	2.80E-10	**27000**	1.01E-07	0	3.10E-08
8000	2.93E-09	0	5.11E-10	**28000**	6.71E-08	0	2.10E-08
9000	4.32E-09	0	9.32E-10	**29000**	4.52E-08	0	1.43E-08
10000	6.48E-09	0	1.69E-09	**30000**	3.11E-08	0	9.89E-09
11000	1.02E-08	0	3.21E-09	**31000**	2.21E-08	0	7.01E-09
12000	1.71E-08	0	6.10E-09	**32000**	1.57E-08	0	4.95E-09
13000	3.07E-08	0	1.15E-08	**33000**	1.14E-08	0	3.50E-09
14000	6.20E-08	0	2.22E-08	**34000**	8.43E-09	0	2.49E-09
15000	1.44E-07	0	4.33E-08	**35000**	6.40E-09	0	1.77E-09
16000	3.89E-07	0	8.15E-08	**36000**	5.05E-09	0	1.28E-09
17000	1.20E-06	0	1.40E-07	**37000**	4.21E-09	0	9.77E-10
18000	4.95E-06	0	1.29E-06	**38000**	3.73E-09	0	8.10E-10
19000	2.80E-05	0	7.08E-05	**39000**	3.42E-09	0	7.13E-10
20000	0.000519	0	1.45E-06	**40000**	3.42E-09	0	7.13E-10

Table 7 : E-field results on Different Antenna Orientation

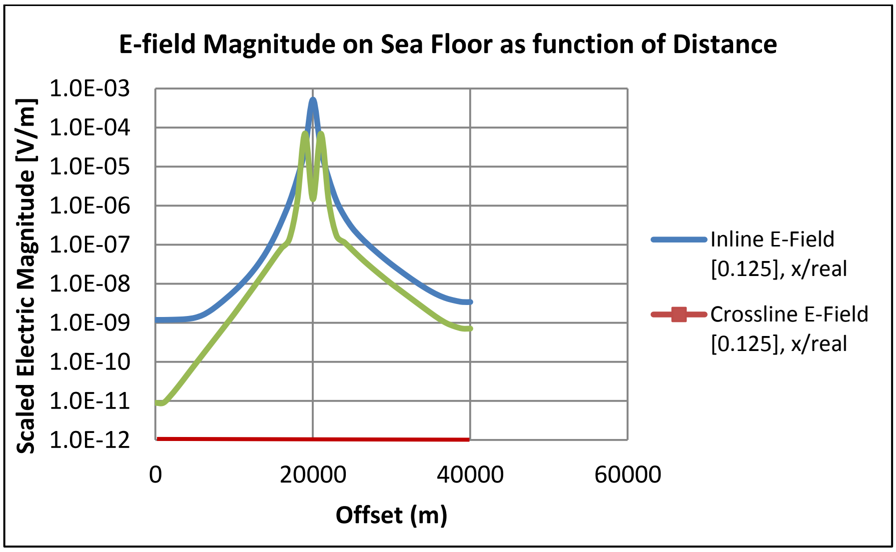

Figure 13 : Graph for electric field magnitude of different antenna orientation.

Result from Figure 13 show the magnitude of received electric field (E-field) from two side area; 0-20000 m of the area without hydrocarbon, and 20000m-40000m which the area with the presence of hydrocarbon. Considering the field received for the case of with hydrocarbon, the magnitude E-field from Horizontal Electric Dipole antenna in line with receiver (HED-R) is showing more higher magnitude compared to electric field received from Vertical Electric Dipole antenna (VED) and Horizontal Electric Dipole antenna, cross line with receiver (HED-P) which is receiving no field from the receiver.

The differences can be observed at the tails of the graph. It was analyzed that HED-R shows a 380% increase in electric field strength as shown in Figure 13. A clearer data for the three antenna is given in Table 7. HED-R is found to be the most suitable antenna in detecting hydrocarbon layer for one layer. Based on the Maxwell equations, the electric field responses of HED-R and VED are as predicted. The electromagnetic wave propagation for HED-R is downward which it is more direct to the hydrocarbon layer whereas for VED, the propagation is on the sideward which is not direct to the target. HED-P is not giving any response because the antenna is not in line with the receiver, which follows the Gauss Law.

$$\Phi_e = \oint \mathbf{E} \cdot d\mathbf{A} = \frac{Q}{\varepsilon_0}$$

$$\Delta\phi_E = E \ \Delta A \ \cos\theta$$

(Gauss Law for Electrostatic)

$$\Phi_B = \oiint_S \mathbf{B} \cdot d\mathbf{S} = 0$$

(Gauss Law for Magnetism)

The electric field for HED-R and VED are in perpendicular to the surface area of receiver on the seabed, whereas the e-field direction for HED-P is parallel to the surface area of the receiver, no field lines pass through at all and the electric flux is zero.

4.1.2 Experiment 2: Varying the thickness of upper hydrocarbon layer

For experiment 2, the previous model had been modified while other parameters are fixed. An upper hydrocarbon layer with the same length has been added to the model. The thickness of upper layer hydrocarbon is varied to obtain the minimum oil layer thickness that EM waves penetrated. The same boundary condition were applied the see the effect of electric field strength within the defined boundary. Figure 3 is the modeling used for the experiment.

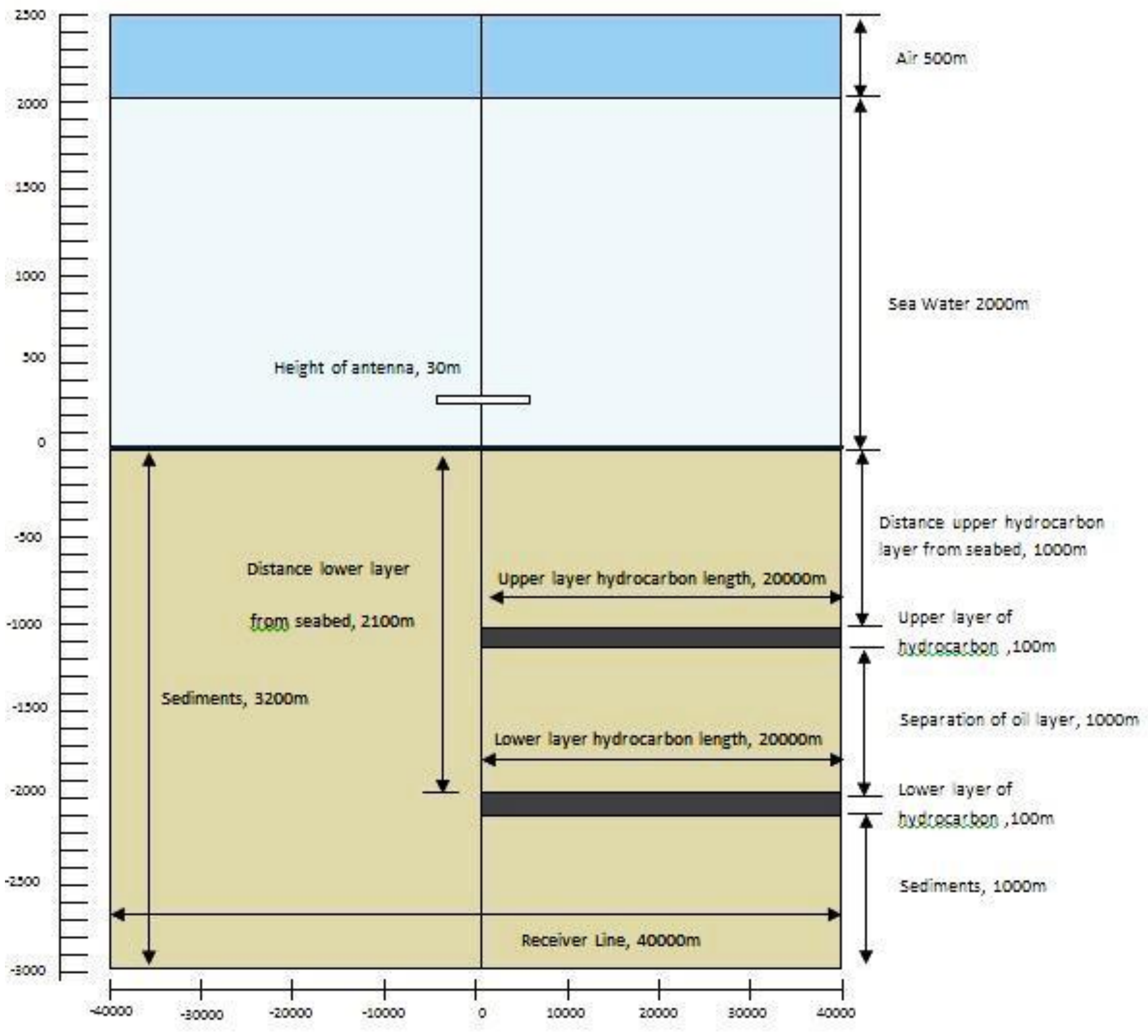

Figure 14: Layer Parameters of Experiment 2

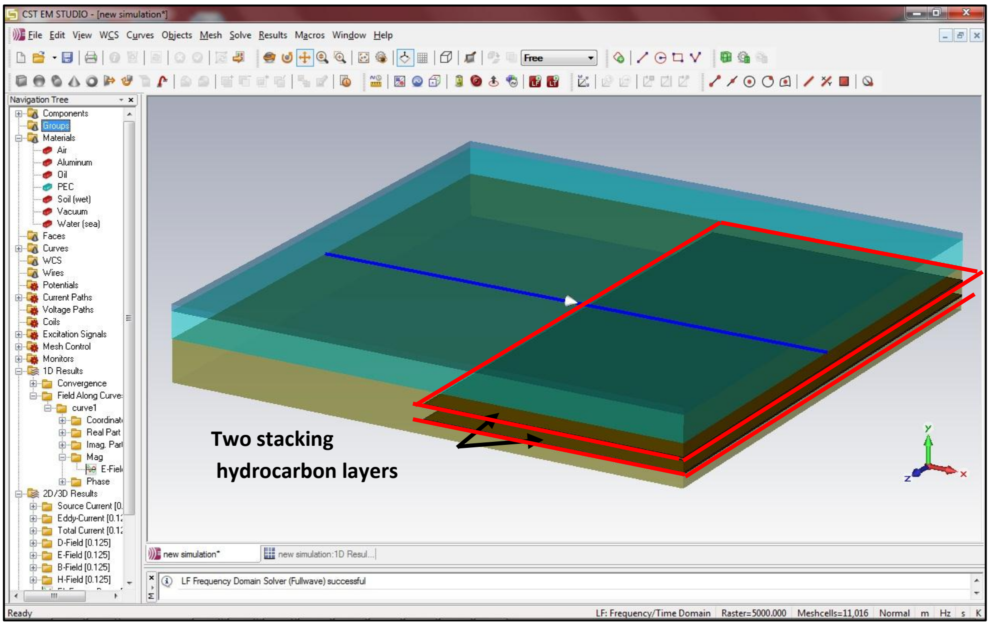

Figure 15 : 3D Modelling Experiment 2 in CST Software

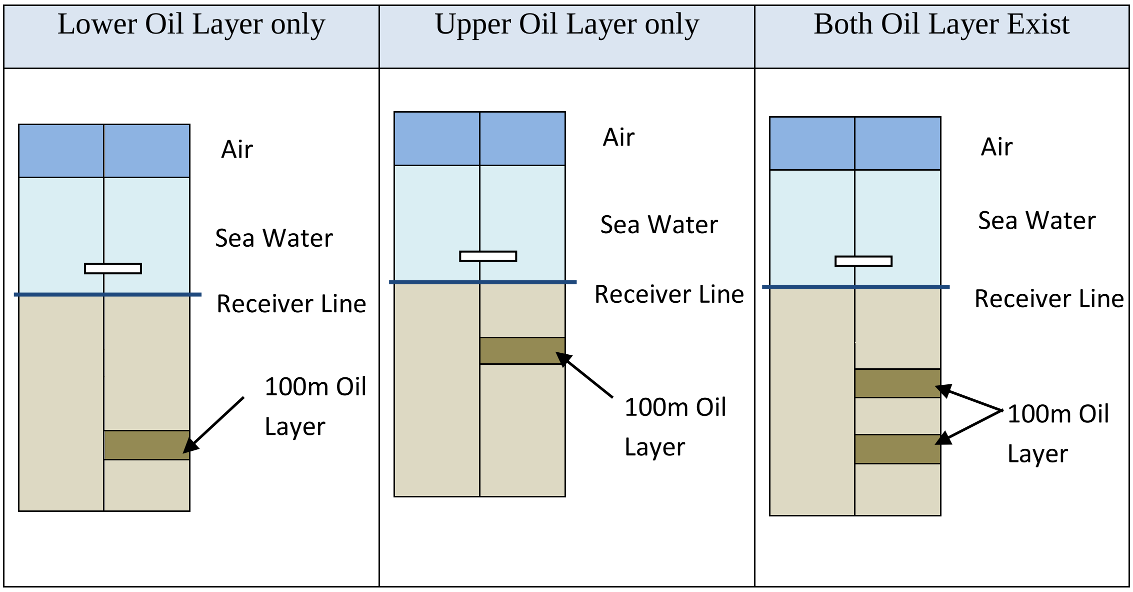

Figure 16 : Experiment 2

By taking the electric field (E-field) magnitude received for lower layer hydrocarbon only, upper layer hydrocarbon only and both hydrocarbon layer as reference, then, the thickness of the upper layer hydrocarbon is varied increasingly; 150m, 200m, 250m, and 500m and decreasingly; 50m, 30m, 20m, 10m, 1m :

Experiment 2 Results – Part 1

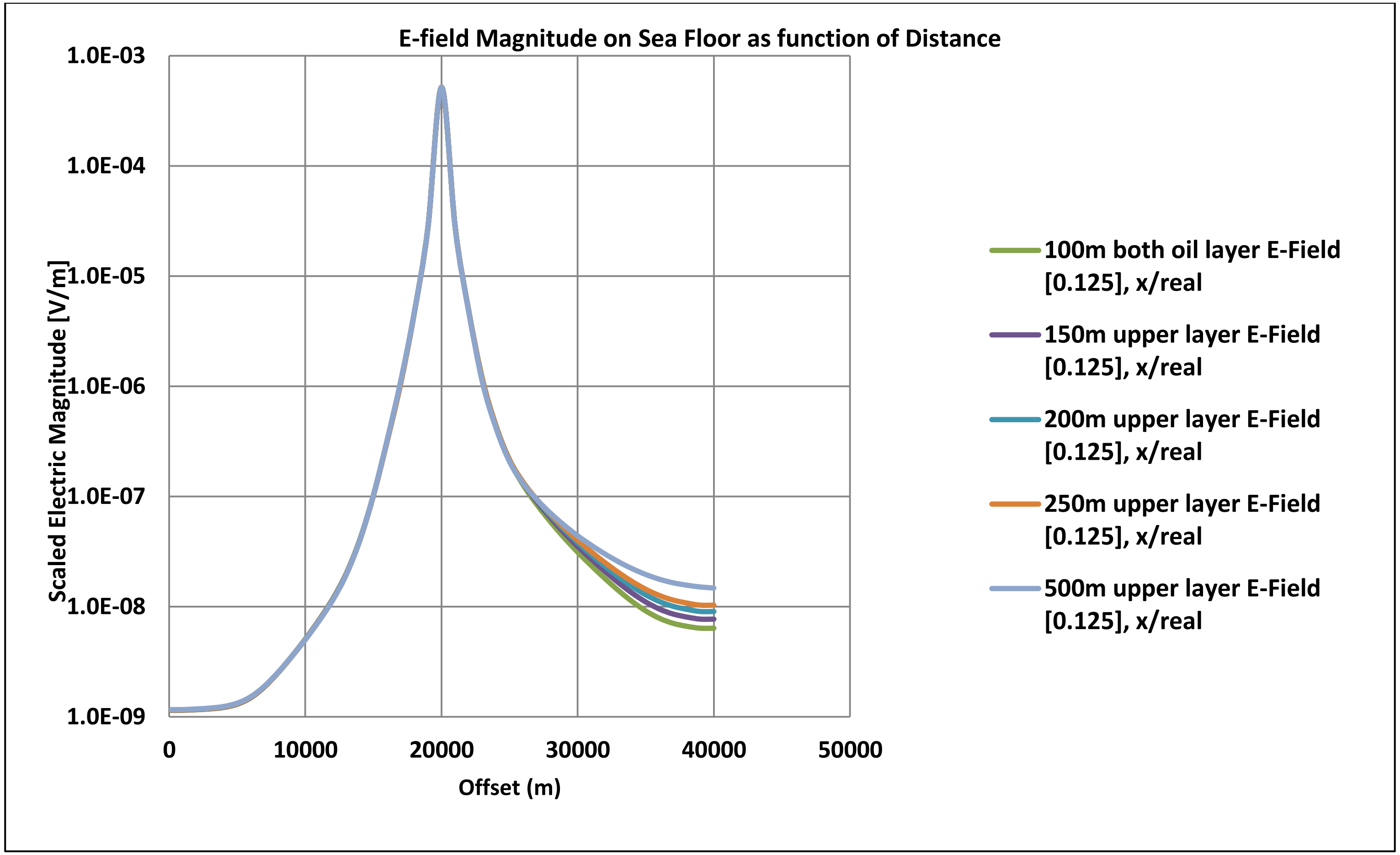

Figure 17 : Graph for electric field Magnitude with increasing thickness of Upper Hydrocarbon layer

Experiment 2 Results – Part 2

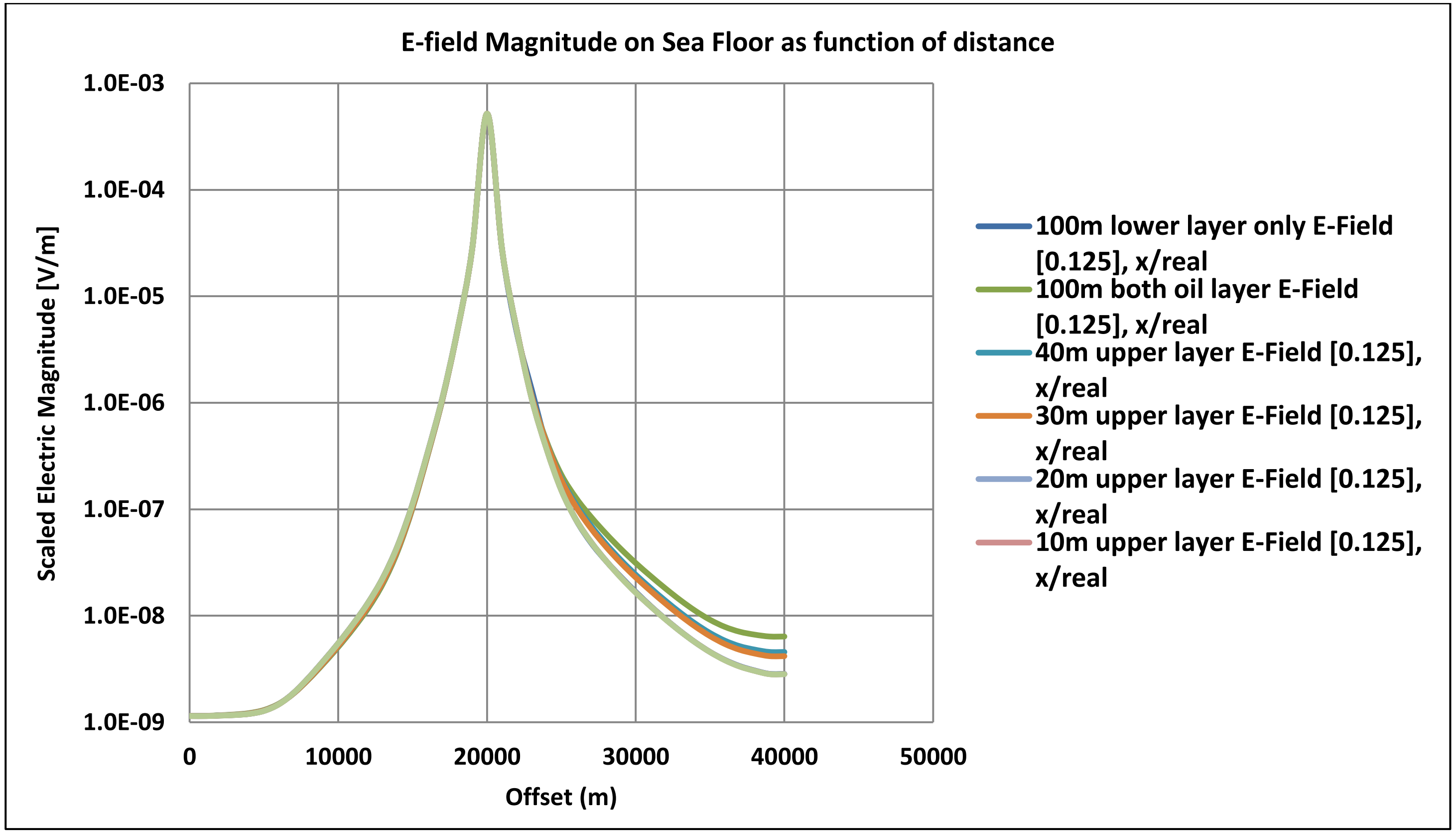

Figure 18 : Graph for electric field Magnitude with decreasing thickness of Upper Hydrocarbon layer

Discussion Part 1 – Increasing Thickness

Offset (m)	100m both oil layer E-Field [0.125], x/real	150m upper layer E-Field [0.125], x/real	250m upper layer E-Field [0.125], x/real	500m upper layer E-Field [0.125], x/real	Offset (m)	100m both oil layer E-Field [0.125], x/real	150m upper layer E-Field [0.125], x/real	250m upper layer E-Field [0.125], x/real	500m upper layer E-Field [0.125], x/real
0	1.15E-09	1.15E-09	1.16E-09	1.17E-09	**21000**	2.74E-05	2.73E-05	2.73E-05	2.69E-05
1000	1.15E-09	1.15E-09	1.16E-09	1.17E-09	**22000**	4.83E-06	4.82E-06	4.81E-06	4.74E-06
2000	1.16E-09	1.17E-09	1.17E-09	1.18E-09	**23000**	1.16E-06	1.15E-06	1.15E-06	1.09E-06
3000	1.18E-09	1.19E-09	1.19E-09	1.20E-09	**24000**	4.34E-07	4.34E-07	4.31E-07	4.16E-07
4000	1.22E-09	1.22E-09	1.23E-09	1.24E-09	**25000**	2.11E-07	2.14E-07	2.14E-07	2.07E-07
5000	1.30E-09	1.31E-09	1.32E-09	1.33E-09	**26000**	1.27E-07	1.32E-07	1.34E-07	1.31E-07
6000	1.50E-09	1.50E-09	1.51E-09	1.53E-09	**27000**	8.43E-08	8.98E-08	9.39E-08	9.35E-08
7000	1.87E-09	1.88E-09	1.88E-09	1.91E-09	**28000**	5.90E-08	6.42E-08	6.89E-08	7.07E-08
8000	2.53E-09	2.53E-09	2.53E-09	2.55E-09	**29000**	4.23E-08	4.70E-08	5.18E-08	5.50E-08
9000	3.57E-09	3.55E-09	3.54E-09	3.56E-09	**30000**	3.12E-08	3.52E-08	3.99E-08	4.39E-08
10000	5.11E-09	5.07E-09	5.04E-09	5.05E-09	**31000**	2.36E-08	2.70E-08	3.15E-08	3.61E-08
11000	7.60E-09	7.53E-09	7.46E-09	7.44E-09	**32000**	1.80E-08	2.09E-08	2.51E-08	3.01E-08
12000	1.18E-08	1.17E-08	1.15E-08	1.15E-08	**33000**	1.40E-08	1.65E-08	2.04E-08	2.55E-08
13000	2.01E-08	1.98E-08	1.96E-08	1.96E-08	**34000**	1.11E-08	1.33E-08	1.69E-08	2.22E-08
14000	4.10E-08	4.06E-08	4.02E-08	4.04E-08	**35000**	9.16E-09	1.10E-08	1.44E-08	1.96E-08
15000	1.04E-07	1.04E-07	1.03E-07	1.04E-07	**36000**	7.85E-09	9.52E-09	1.26E-08	1.78E-08
16000	3.19E-07	3.18E-07	3.17E-07	3.24E-07	**37000**	7.08E-09	8.59E-09	1.15E-08	1.65E-08
17000	1.08E-06	1.08E-06	1.08E-06	1.13E-06	**38000**	6.65E-09	8.06E-09	1.08E-08	1.57E-08
18000	4.75E-06	4.75E-06	4.74E-06	4.79E-06	**39000**	6.39E-09	7.72E-09	1.03E-08	1.51E-08
19000	2.77E-05	2.77E-05	2.77E-05	2.81E-05	**40000**	6.39E-09	7.72E-09	1.03E-08	1.48E-08
20000	0.000518	0.000518	0.00051	0.000519					

Table 8 : E-field results on increasing thickness of upper layer hydrocarbon

From Figure 17, the graph obtained, there are different response of E-field when the thickness of the upper hydrocarbon layer been increased. The left side of the graph (offset of 0m to 20000m), represents the case where no oil layer presence. It is showing a low magnitude of electric field. On the other hand, in Table 8, the magnitude of E-field is increasing with respect to the increasing thickness of the upper hydrocarbon layer.

For the thickness 150m of hydrocarbon layer, $\frac{7.72\text{E}-09-6.39\text{E}-09}{6.39\text{E}-09}$ x 100 = 20.81%

For the thickness 250m of hydrocarbon layer, $\frac{1.03\text{E}-08-6.39\text{E}-09}{6.39\text{E}-09}$ x 100 = 61.78%

For the thickness 500m of hydrocarbon layer, $\frac{1.48\text{E}-08-6.39\text{E}-09}{6.39\text{E}-09}$ x 100 = 131.61%

The increasing precentange with respect to increasing thickness of upper hydrocarbon layer, this clearly show that the magnitude of E-field increase when the thickness increase. The transmitter is detecting only the upper layer of the hydrocarbon. The lower layer of hydrocarbon is been neglected.

Discussion Part 2 – Decreasing Thickness

Length	100m lower layer only E-Field [0.125], x/real	100m both oil layer E-Field [0.125], x/real	Both layer exist				
			40m upper layer E-Field [0.125], x/real	30m upper layer E-Field [0.125], x/real	20m upper layer E-Field [0.125], x/real	10m upper layer E-Field [0.125], x/real	1m upper layer E-Field [0.125], x/real
0	1.15E-09	1.15E-09	1.15E-09	1.15E-09	1.15E-09	1.14E-09	1.14E-09
1000	1.15E-09	1.15E-09	1.15E-09	1.15E-09	1.15E-09	1.14E-09	1.14E-09
2000	1.16E-09	1.16E-09	1.16E-09	1.16E-09	1.16E-09	1.15E-09	1.15E-09
3000	1.17E-09	1.18E-09	1.18E-09	1.18E-09	1.17E-09	1.17E-09	1.17E-09
4000	1.20E-09	1.22E-09	1.21E-09	1.21E-09	1.20E-09	1.20E-09	1.20E-09
5000	1.28E-09	1.30E-09	1.29E-09	1.29E-09	1.28E-09	1.28E-09	1.28E-09
6000	1.48E-09	1.50E-09	1.49E-09	1.49E-09	1.48E-09	1.48E-09	1.48E-09
7000	1.90E-09	1.87E-09	1.87E-09	1.87E-09	1.89E-09	1.89E-09	1.89E-09
8000	2.63E-09	2.53E-09	2.55E-09	2.55E-09	2.62E-09	2.62E-09	2.62E-09
9000	3.79E-09	3.57E-09	3.61E-09	3.63E-09	3.78E-09	3.78E-09	3.78E-09
10000	5.55E-09	5.11E-09	5.21E-09	5.24E-09	5.53E-09	5.53E-09	5.53E-09
11000	8.42E-09	7.60E-09	7.80E-09	7.87E-09	8.40E-09	8.40E-09	8.40E-09
12000	1.33E-08	1.18E-08	1.22E-08	1.23E-08	1.33E-08	1.33E-08	1.33E-08
13000	2.29E-08	2.01E-08	2.08E-08	2.10E-08	2.28E-08	2.28E-08	2.28E-08
14000	4.62E-08	4.10E-08	4.22E-08	4.26E-08	4.60E-08	4.60E-08	4.60E-08
15000	1.15E-07	1.04E-07	1.07E-07	1.07E-07	1.14E-07	1.14E-07	1.14E-07
16000	3.40E-07	3.19E-07	3.23E-07	3.25E-07	3.38E-07	3.38E-07	3.38E-07
17000	1.13E-06	1.08E-06	1.09E-06	1.09E-06	1.12E-06	1.12E-06	1.12E-06
18000	4.87E-06	4.75E-06	4.77E-06	4.77E-06	4.83E-06	4.83E-06	4.83E-06
19000	2.81E-05	2.77E-05	2.78E-05	2.78E-05	2.79E-05	2.79E-05	2.79E-05
20000	0.000517	0.00052	0.000519	0.000519	0.000517	0.000518	0.000518
21000	2.72E-05	2.74E-05	2.74E-05	2.75E-05	2.75E-05	2.75E-05	2.75E-05
22000	4.57E-06	4.83E-06	4.84E-06	4.84E-06	4.78E-06	4.78E-06	4.77E-06

23000	1.33E-06	1.16E-06	1.16E-06	1.15E-06	1.09E-06	1.09E-06	1.09E-06
24000	3.96E-07	4.34E-07	4.23E-07	4.17E-07	3.67E-07	3.66E-07	3.65E-07
25000	1.53E-07	2.11E-07	1.94E-07	1.88E-07	1.51E-07	1.51E-07	1.50E-07
26000	7.86E-08	1.27E-07	1.10E-07	1.04E-07	7.93E-08	7.91E-08	7.89E-08
27000	4.81E-08	8.43E-08	6.95E-08	6.56E-08	4.90E-08	4.89E-08	4.88E-08
28000	3.27E-08	5.90E-08	4.73E-08	4.45E-08	3.29E-08	3.28E-08	3.28E-08
29000	2.32E-08	4.23E-08	3.33E-08	3.13E-08	2.29E-08	2.29E-08	2.28E-08
30000	1.67E-08	3.12E-08	2.42E-08	2.28E-08	1.65E-08	1.65E-08	1.64E-08
31000	1.24E-08	2.36E-08	1.82E-08	1.71E-08	1.23E-08	1.23E-08	1.23E-08
32000	9.30E-09	1.80E-08	1.38E-08	1.30E-08	9.28E-09	9.27E-09	9.25E-09
33000	7.14E-09	1.40E-08	1.07E-08	1.00E-08	7.14E-09	7.13E-09	7.12E-09
34000	5.64E-09	1.11E-08	8.46E-09	7.93E-09	5.64E-09	5.63E-09	5.63E-09
35000	4.57E-09	9.16E-09	6.88E-09	6.43E-09	4.57E-09	4.56E-09	4.56E-09
36000	3.84E-09	7.85E-09	5.83E-09	5.42E-09	3.83E-09	3.82E-09	3.82E-09
37000	3.37E-09	7.08E-09	5.18E-09	4.79E-09	3.35E-09	3.34E-09	3.34E-09
38000	3.06E-09	6.65E-09	4.81E-09	4.42E-09	3.05E-09	3.04E-09	3.04E-09
39000	2.85E-09	6.39E-09	4.57E-09	4.18E-09	2.84E-09	2.83E-09	2.83E-09
40000	2.85E-09	6.39E-09	4.57E-09	4.18E-09	2.84E-09	2.83E-09	2.83E-09

Table 9 : E-field results on decreasing thickness of upper layer hydrocarbon

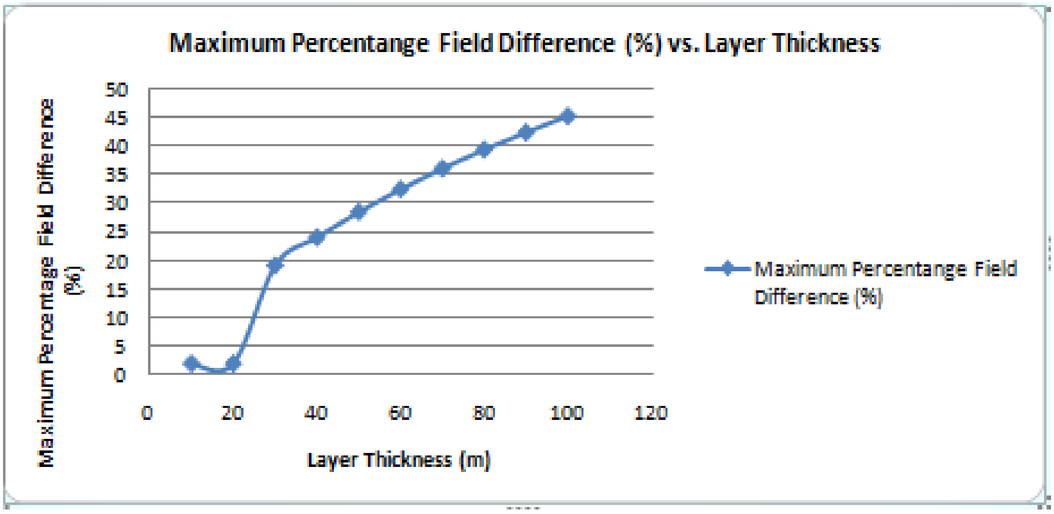

Figure 18 : Maximum Percentange Difference vs. Layer Thickness (m)

From the graph obtained, as in experiment 2.1, there are different responses between thickness of layers. On the left side of the graph (0-40000m), represents the case of without hydrocarbon layer. For the right side of the graph, the response for 20m, 10m, and 1m of upper layer hydrocarbon is the same as if there is only lower layer of hydrocarbon in the modelling. However, when the thickness of the upper layer hydrocarbon increase to 30m, the magnitude of E-field deviates from the E field response of 20m, 10m, and 1m of the upper layer hydrocarbon.

For 1m of upper hydrocarbon layer, $\frac{2.83\mathrm{E}{-}09 - 2.85\mathrm{E}{-}09}{2.85\mathrm{E}{-}09}$ x 100 = -0.7%

For 10m of upper hydrocarbon layer, $\frac{2.83\mathrm{E}{-}09 - 2.85\mathrm{E}{-}09}{2.85\mathrm{E}{-}09}$ x 100 = -0.7%

For 20m of upper hydrocarbon layer, $\frac{2.84\mathrm{E}{-}09 - 2.85\mathrm{E}{-}09}{2.85\mathrm{E}{-}09}$ x 100 = -0.35%

For 30m of upper hydrocarbon layer, $\frac{4.18\mathrm{E}{-}09 - 2.85\mathrm{E}{-}09}{2.85\mathrm{E}{-}09}$ x 100 = 46%

For 40m of upper hydrocarbon layer, $\frac{4.57\mathrm{E}{-}09 - 2.85\mathrm{E}{-}09}{2.85\mathrm{E}{-}09}$ x 100 = 60.35%

Based on the difference obtained in the calculation, the magnitude of E-field deviates more at the upper layer hydrocarbon thickness of 30m. This may also relates with the concept of skin depth where

$$\delta = \sqrt{\frac{2}{\mu\omega\sigma}},$$

it shows how far EM waves penetrate into a medium. If the skin depth is large for high resistive medium, it will have higher rate of attenuation as compared to the low resistive medium. Based on the calculation for skin depth, 780m in seawater (0.3Ωm), 2013m in 2Ωm of sediments, and 4E+08 in air for 0.125Hz.

4.1.3 *Experiment 3: Varying position of 2nd Hydrocarbon Layer*

In experiment 3, the length of upper layer hydrocarbon is been reduced to 5000m. The author also varies the position of upper layer to observe the response of electric field magnitude with respect to different placement of hydrocarbon layer. Percentange difference of electric field magnitude between the cases where lower layer only exist and both oil layer presence as in Figure 30 are being recorded. All other parameters are fixed.

Figure 19: Case 1 – HC Offset (20000-25000)

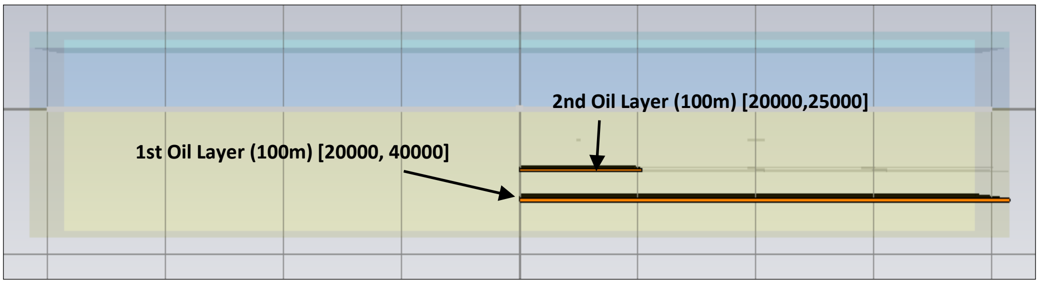

- **Figure 20: Case 2 – HC Offset (25000-30000)**

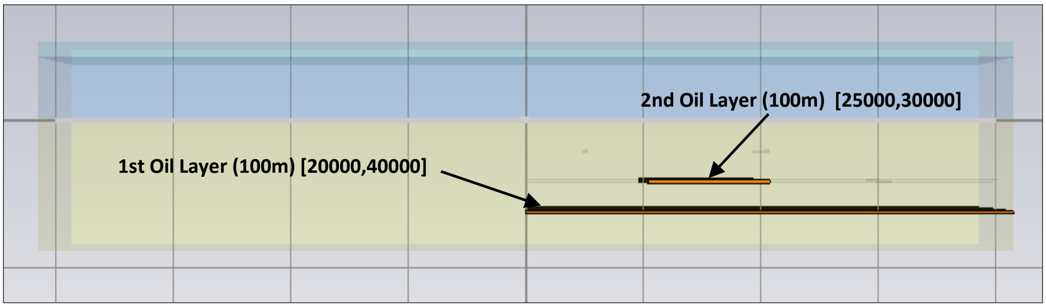

- **Figure 21: Case 3 – HC Offset (30000-35000)**

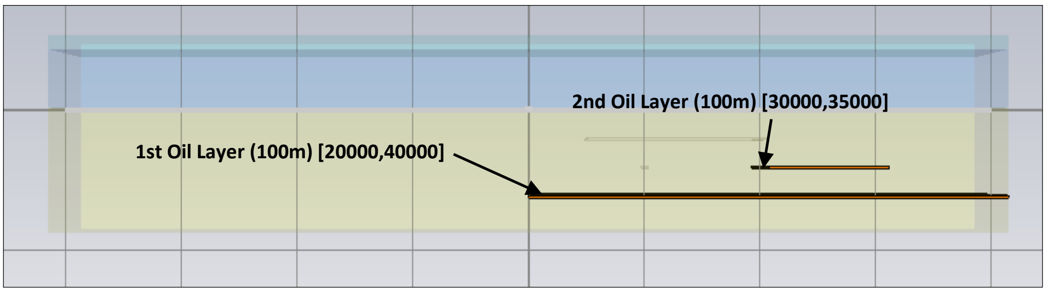

- **Figure 22: Case 4- HC Offset (35000-40000)**

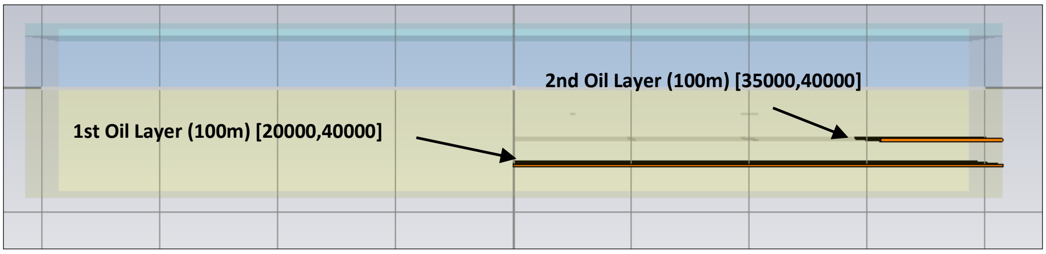

Results Experiment 3

Case 1 – HC Offset (20000-25000)

Offset(m)	E-Value Without 2nd Layer (V/m)	E-Value With 2nd Layer (V/m)	Percentage Differences (%)
2.00E+04	0.000555241	0.00055528	0.007132045
2.10E+04	3.10E-05	3.10E-05	-0.171954119
2.20E+04	5.24E-06	5.23E-06	-0.182736509
2.30E+04	1.46E-06	1.49E-06	1.674281808
2.40E+04	4.17E-07	4.53E-07	8.678763525
2.50E+04	1.31E-07	1.60E-07	22.29764484
2.60E+04	5.51E-08	7.09E-08	28.70007188
2.70E+04	3.05E-08	3.79E-08	24.3630459
2.80E+04	2.00E-08	2.39E-08	19.44423881
2.90E+04	1.40E-08	1.63E-08	16.1029573
3.00E+04	1.02E-08	1.17E-08	14.32000422
3.10E+04	7.58E-09	8.60E-09	13.45414978
3.20E+04	5.72E-09	6.47E-09	13.09529574
3.30E+04	4.48E-09	5.00E-09	11.55596232
3.40E+04	3.58E-09	3.94E-09	10.00827559
3.50E+04	2.92E-09	3.20E-09	9.355858445
3.60E+04	2.45E-09	2.68E-09	9.622044233
3.70E+04	2.10E-09	2.32E-09	10.15408937
3.80E+04	1.89E-09	2.07E-09	9.937118124
3.90E+04	1.77E-09	1.94E-09	9.558899292
4.00E+04	1.72E-09	1.89E-09	9.476069579

2nd Oil Layer (gray)	20000m-25000m
Oil Shown at Receiver (tan)	23000m-26000m
Range Percentage Field Difference	1.7% - 28%

Case 2 – HC Offset (25000-30000)

Offset(m)	E-Value Without 2nd Layer (V/m)	E-Value With 2nd Layer (V/m)	Percentage Differences (%)
2.00E+04	0.000555241	0.00055524	-3.60204E-05
2.10E+04	3.10E-05	3.10E-05	0.001384909
2.20E+04	5.24E-06	5.24E-06	0.007869493
2.30E+04	1.46E-06	1.46E-06	0.008143194
2.40E+04	4.17E-07	4.16E-07	-0.223595082
2.50E+04	1.31E-07	1.29E-07	-1.863052071
2.60E+04	5.51E-08	5.25E-08	-4.645927729
2.70E+04	3.05E-08	3.02E-08	-1.062292009
2.80E+04	2.00E-08	2.13E-08	6.54055314
2.90E+04	1.40E-08	1.59E-08	12.87165655
3.00E+04	1.02E-08	1.17E-08	14.3462834
3.10E+04	7.58E-09	8.58E-09	13.17602977
3.20E+04	5.72E-09	6.43E-09	12.31889999
3.30E+04	4.48E-09	4.94E-09	10.29398342
3.40E+04	3.58E-09	3.87E-09	8.016132521
3.50E+04	2.92E-09	3.11E-09	6.432417823
3.60E+04	2.45E-09	2.59E-09	5.753010719
3.70E+04	2.10E-09	2.22E-09	5.373033814
3.80E+04	1.89E-09	1.97E-09	4.426920103
3.90E+04	1.77E-09	1.83E-09	3.578614479
4.00E+04	1.72E-09	1.78E-09	3.313264373

2nd Oil Layer (gray)	25000m-30000m
Oil Shown at Receiver (tan)	28000m-31000m
Range Percentage Field Difference	6.5% - 13.9%

Case 3 – HC Offset (30000-35000)

Offset(m)	E-Value Without 2nd Layer (V/m)	E-Value With 2nd Layer (V/m)	Percentage Differences (%)
2.00E+04	0.000555241	0.000555241	1.80102E-05
2.10E+04	3.10E-05	3.10E-05	0
2.20E+04	5.24E-06	5.24E-06	5.73021E-05
2.30E+04	1.46E-06	1.46E-06	0.000752732
2.40E+04	4.17E-07	4.17E-07	0.006184341
2.50E+04	1.31E-07	1.31E-07	0.0340621
2.60E+04	5.51E-08	5.52E-08	0.085379399
2.70E+04	3.05E-08	3.05E-08	0.001999007
2.80E+04	2.00E-08	1.99E-08	-0.525359093
2.90E+04	1.40E-08	1.38E-08	-1.868571933
3.00E+04	1.02E-08	9.86E-09	-3.650383344

3.10E+04	7.58E-09	7.27E-09	-4.108475383
3.20E+04	5.72E-09	5.66E-09	-0.998118226
3.30E+04	4.48E-09	4.66E-09	3.973577624
3.40E+04	3.58E-09	3.88E-09	8.430247082
3.50E+04	2.92E-09	3.21E-09	9.882140022
3.60E+04	2.45E-09	2.66E-09	8.798498767
3.70E+04	2.10E-09	2.25E-09	6.935805054
3.80E+04	1.89E-09	1.98E-09	5.221030482
3.90E+04	1.77E-09	1.84E-09	4.127655045
4.00E+04	1.72E-09	1.79E-09	3.698762495

2nd Oil Layer (gray)	30000m-35000m
Oil Shown at Receiver (tan)	33000m-35000m
Range Percentage Field Difference	3.4% - 9.9%

Case 4- HC Offset (35000-40000)

Offset(m)	E-Value Without 2nd Layer (V/m)	E-Value With 2nd Layer (V/m)	Percentage Differences (%)
2.00E+04	0.000555241	0.000555241	0
2.10E+04	3.10E-05	3.10E-05	0
2.20E+04	5.24E-06	5.24E-06	-1.91007E-05
2.30E+04	1.46E-06	1.46E-06	0
2.40E+04	4.17E-07	4.17E-07	-0.000119852
2.50E+04	1.31E-07	1.31E-07	0.000152403
2.60E+04	5.51E-08	5.51E-08	0.002522367
2.70E+04	3.05E-08	3.05E-08	0.008946376
2.80E+04	2.00E-08	2.00E-08	0.018007167
2.90E+04	1.40E-08	1.40E-08	0.024352245
3.00E+04	1.02E-08	1.02E-08	0.011723055
3.10E+04	7.58E-09	7.57E-09	-0.055288839
3.20E+04	5.72E-09	5.71E-09	-0.238538701
3.30E+04	4.48E-09	4.45E-09	-0.642393413
3.40E+04	3.58E-09	3.54E-09	-1.320968789
3.50E+04	2.92E-09	2.87E-09	-1.89855489
3.60E+04	2.45E-09	2.41E-09	-1.424586164
3.70E+04	2.10E-09	2.13E-09	1.140296517
3.80E+04	1.89E-09	1.97E-09	4.304210827
3.90E+04	1.77E-09	1.88E-09	6.595450289
4.00E+04	1.72E-09	1.85E-09	7.533258861

2nd Oil Layer (gray)	35000m-40000m
Oil Shown at Receiver (tan)	37000m-40000m
Range Percentage Field Difference	1.1% - 7.5%

Analysis

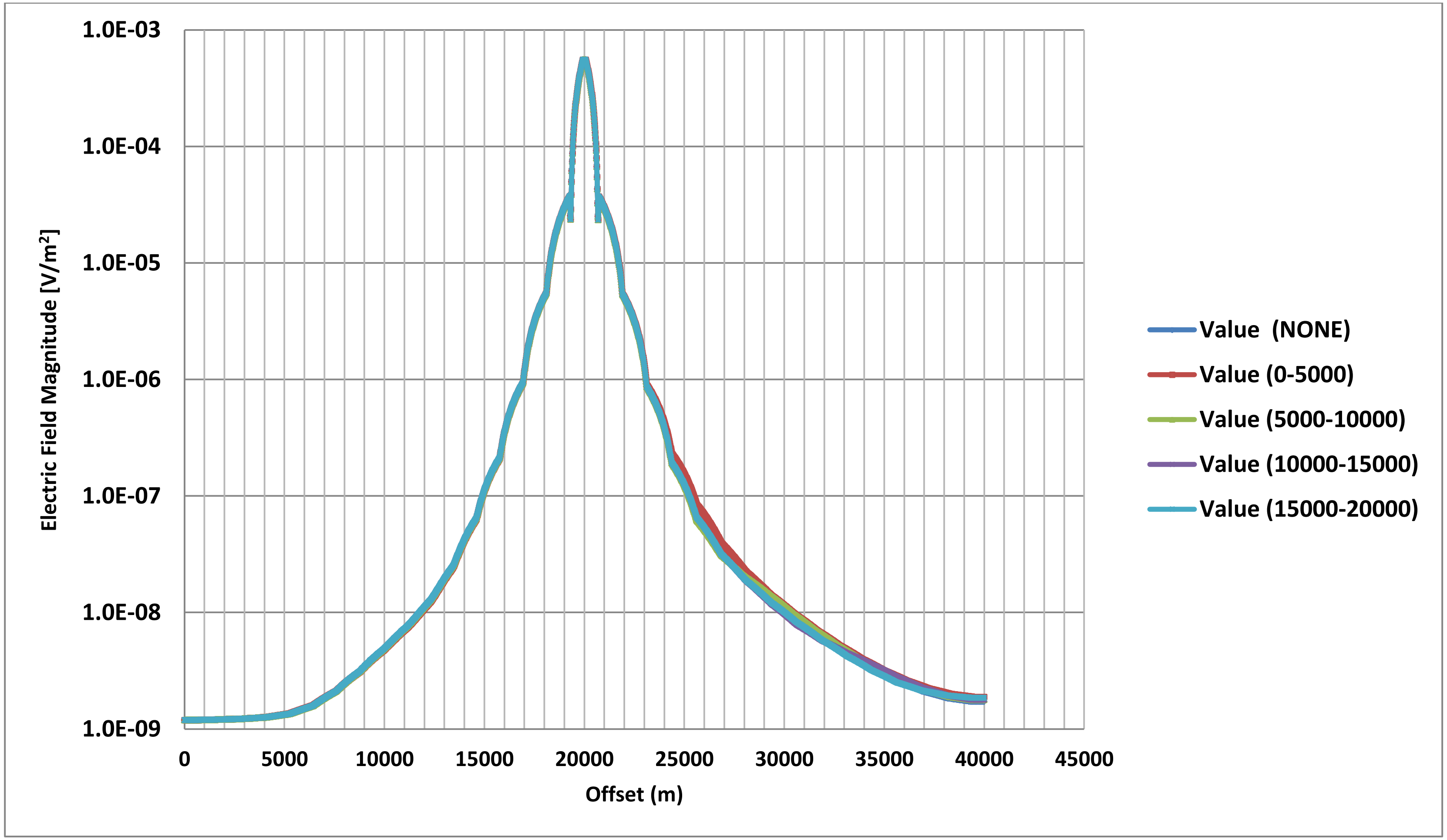

Figure 23 : Responses of E-field for Experiment 3

Percentage Difference Comparison

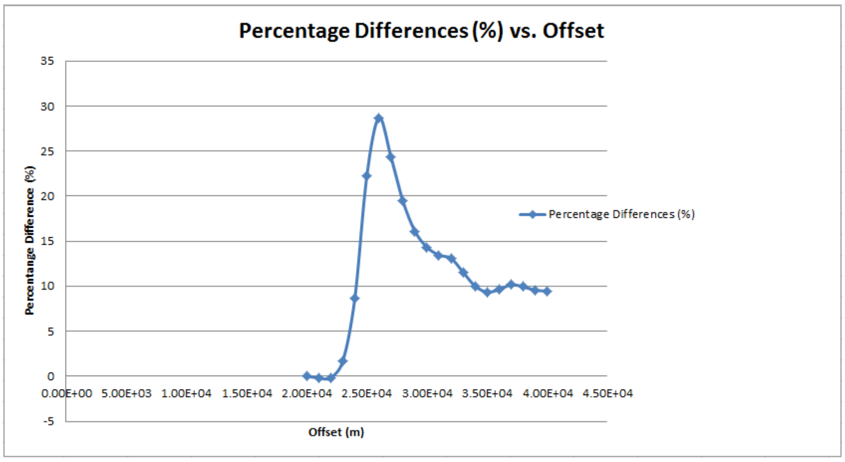

Figure 24 : Case 1 – HC Offset : 20000-25000

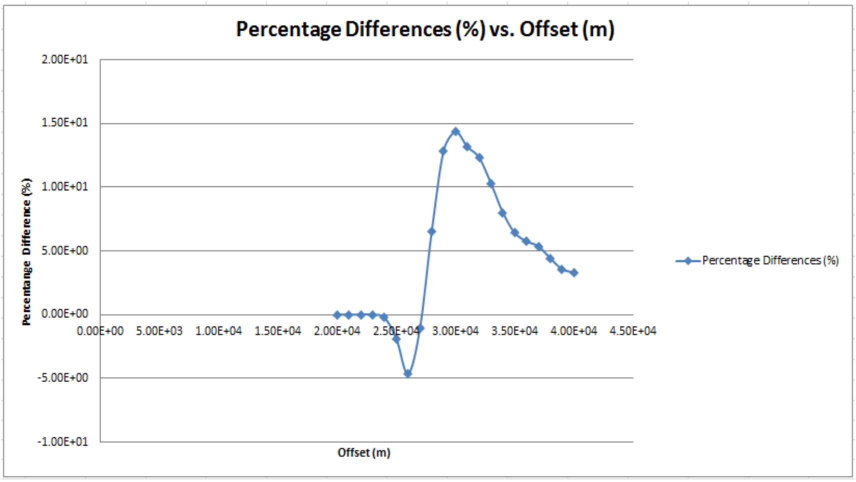

Figure 25 : Case 2 – HC Offset : 25000-30000

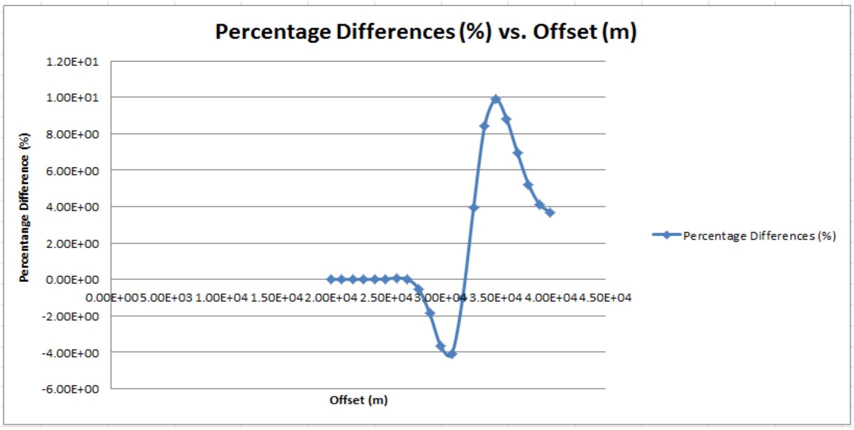

Figure 26 : Case 3 – HC Offset : 30000-35000

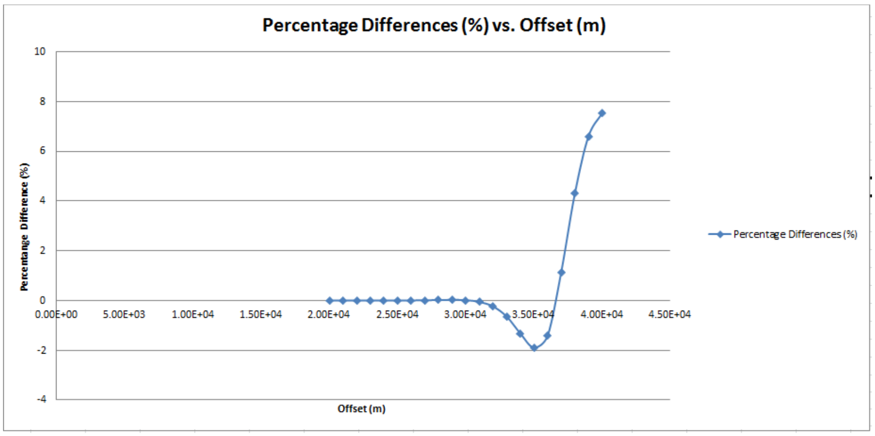

Figure 27 : Case 4- HC Offset : 35000-40000

In different cases, the original location of oil layer is being highlighted with gray and oil being shown at certain offset (tan). In the graph obtained, there are slight different responses between location of second hydrocarbon layer. Responses are taken on the right side of the model (20000-40000m), for two layers, varying the position of second layer hydrocarbon as shown above. Comparing the percentage difference between the simulations done as in Figure 16, the minimum percentage of starting point of hydrocarbon to be considered is 1% and the highest percentage field difference is taken as the ending point of hydrocarbon for every cases.

It is shown in the result that the percentage of E field increased as minimum as 1% after 3000m the original location of hydrocarbon. It can be interpreted that the oil location can be determined to be in the 3000m earlier after the first receiver detects minimum percentage difference of 1% to the highest percentage difference where it can be assumed as the ending point of the second hydrocarbon layer.

4.1.4 Experiment 4: Fixed position of two layer hydrocarbon

In this experiment, the position of the upper layer hydrocarbon is fixed and different antennas in the Figure 10 and 12 are used to find the best oriented antenna to detect stacking of hydrocarbon layer in the seabed. Percentange difference of Electric field magnitude between the case where lower layer only exist and both oil layer presence as in Figure 30 are being recorded. Both antenna are being compared. Figure 28 is the modeling used for the experiment.

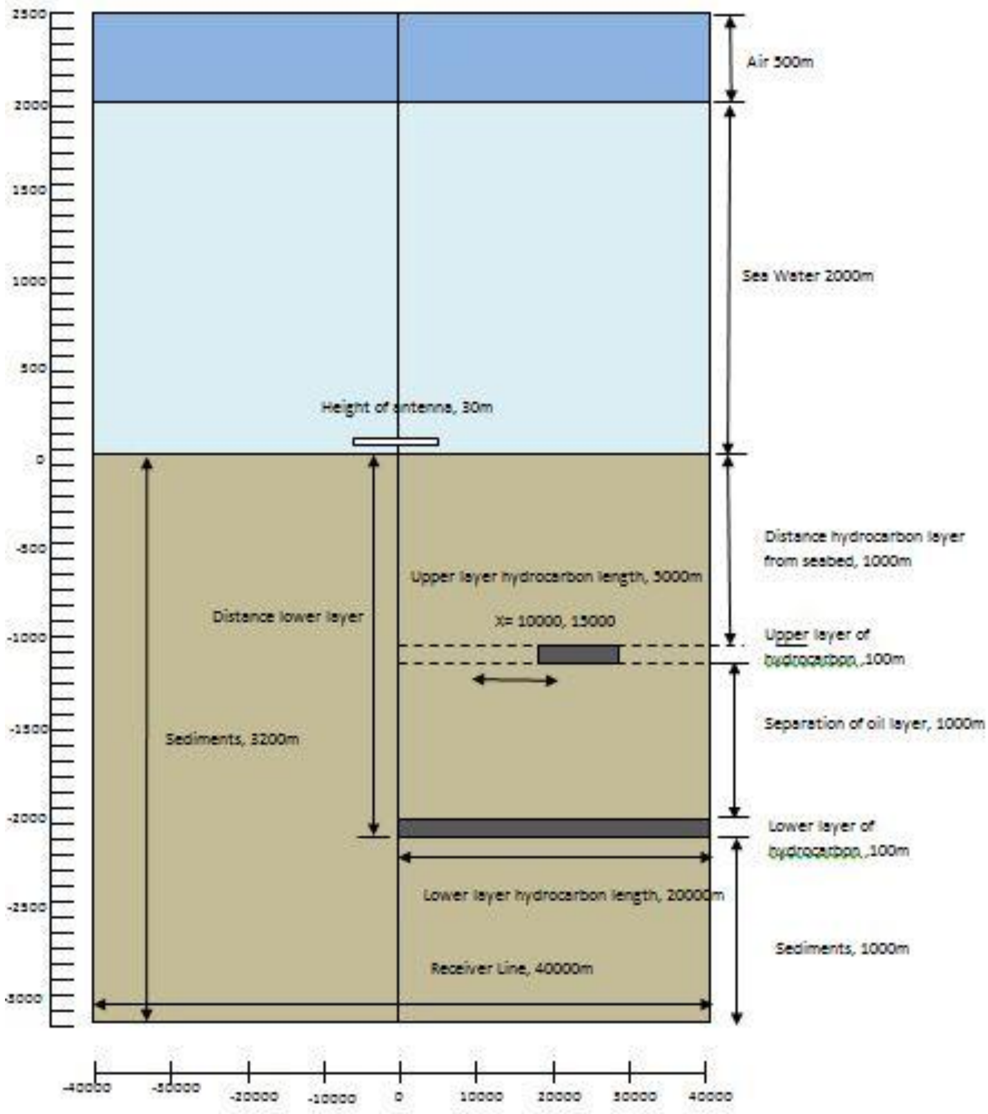

Figure 28 : Layer Parameters of Experiment 4

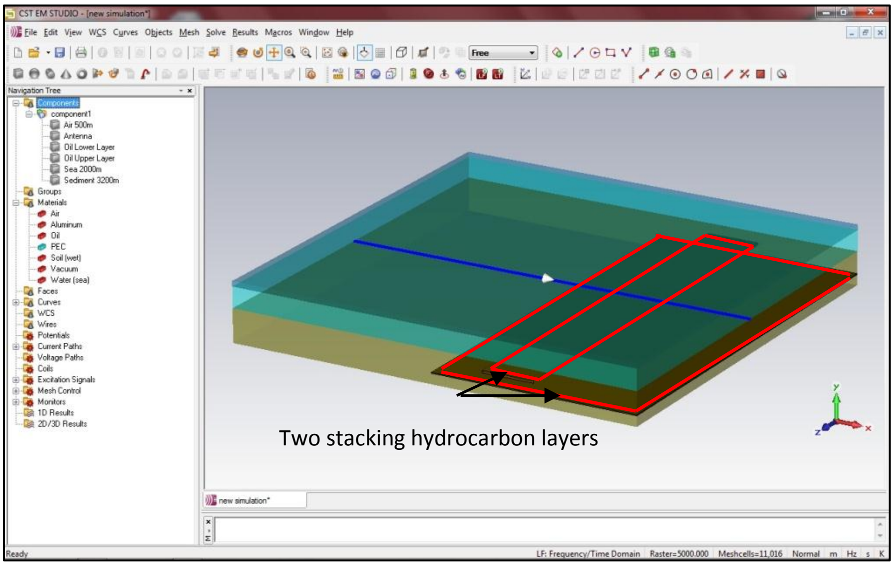

Figure 29 : 3D Modelling in CST Software

Lower Oil Layer only	Both Oil Layer Exist
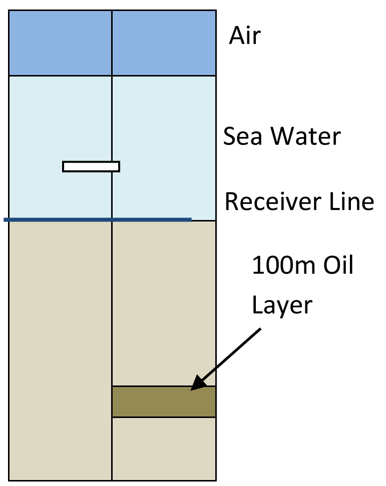	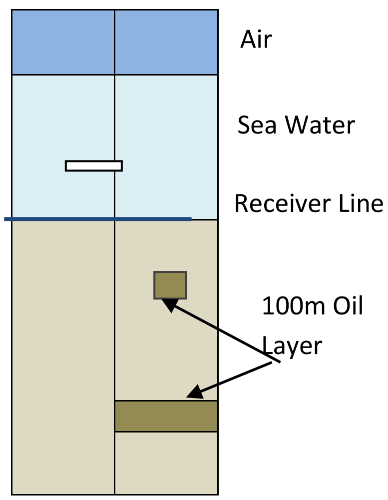

Figure 30 : Experiment 4

Results Experiment 4

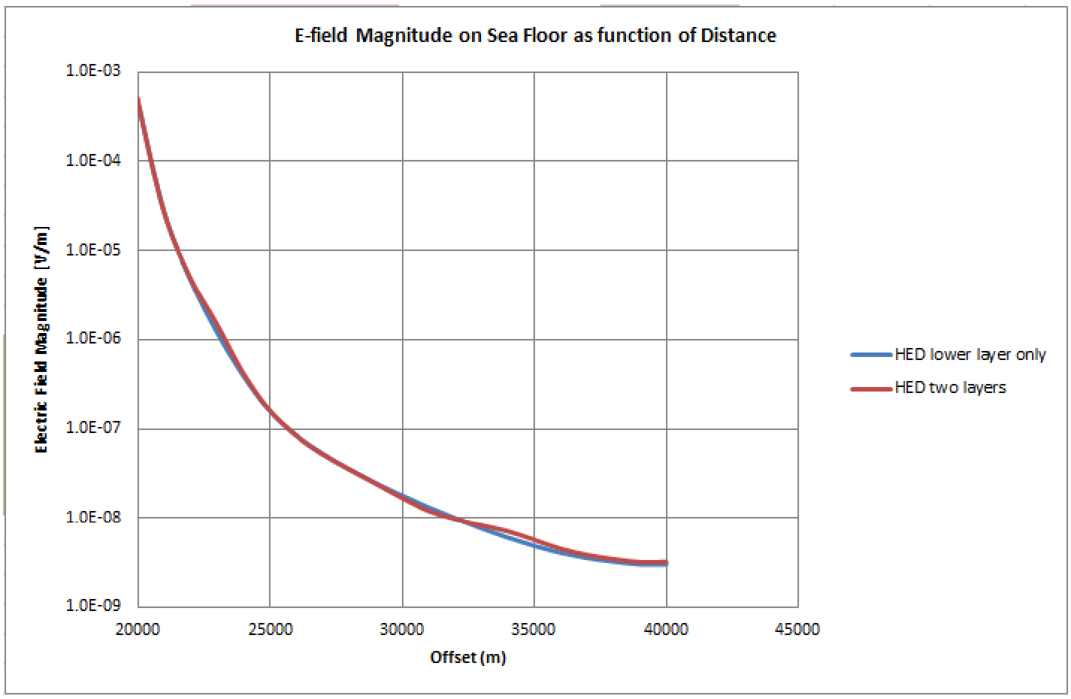

Figure 31: Electric field response for Horizontal Electric Dipole Antena, Inline with receiver (HED-R)

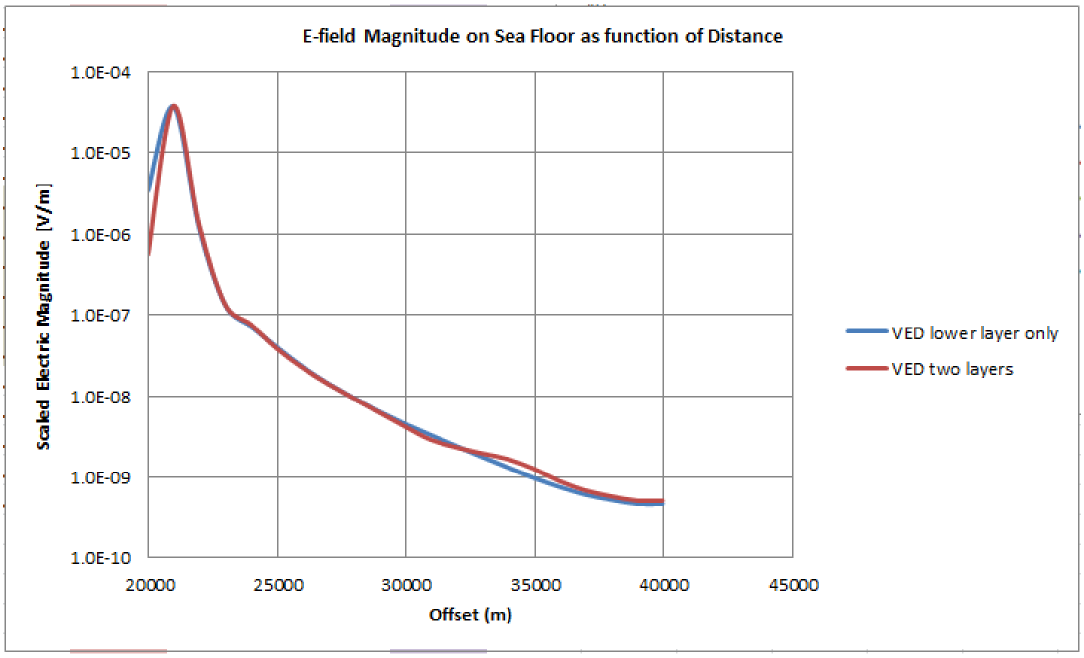

Figure 32 : Electric field response for Vertical Electric Dipole Antena (VED)

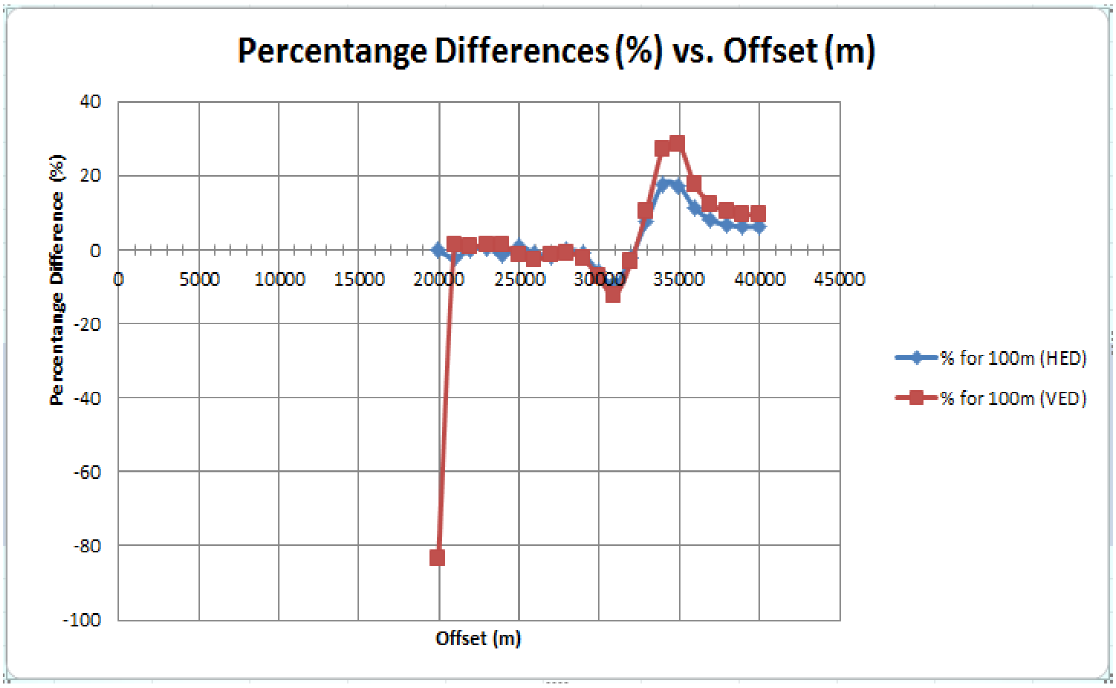

Figure 33 : Percentage Difference between HED and VED

CONDITION	HED (INLINE)	VED
1st Hydrocarbon layer only exist.	4.90E-09	9.78E-10
Both layers exist	5.74E-09	1.26E-09
Percentange Difference (%)	17.12	28.33

Table 10 : Percentage Difference between HED and VED

In Figure 31 and 32, there are different responses obtained for both cases. Figure 31 shows the electric field response for HED-R antenna and Figure 32 shows the electric field response for VED antenna. The blue lines represent the electric field response for only one layer presence in the model whereas the red lines represent the electric field response for both layer exist (Refer to figure 30) . The differences can be observed in both graphs which are from offset 30000-35000m. This is due to location of the hydrocarbon is at the distance of 10000-15000m. There are different detection responses between two different antennas which are Horizontal Electric Dipole, in line with the receivers (HED-R) and Vertical Electric Dipole (VED)

In the experiment, Vertical Electric Dipole (VED) gives the highest increment in percentage detecting double stacking up to 11.21%. Based on the Maxwell theories for antenna, and field propagation, it can be interpreted that VED is the best antenna orientation to detect double layer of hydrocarbon.

CHAPTER 5

CONCLUSION

5.1 Conclusion

In a nutshell, this project is a comprehensive research study about comparison of antenna orientations and variation of thickness and position of two hydrocarbon layers in seabed logging. The author believes that this project will be beneficial to the future of oil and gas industry. To conclude, the Vertical Electric Dipole (VED) is the best oriented antenna to detect stacks of hydrocarbon layer with an increase of 11.21% percentage difference as compared to Horizontal Electric Dipole (HED) antenna in Seabed Logging. The thickness variation of hydrocarbon layers shows that for every increment of 50m upper oil layer, there will be 20% increment of E-field magnitude, recorded by the receiver. The minimum thickness of upper hydrocarbon layer to block the response of lower hydrocarbon layer is 30m. The thicker oil layer, the higher E-field obtained. The oil location can be determine by observing the increase of percentage difference.

5.2 Recommendation

Improvement on developed SBL Simulator can be done by including more inputs parameter option that consider all size and shape of hydrocarbon reservoir including the shape of antenna. Frequency variation also vary the response of E-field received. Higher dimension modeling can be developed for better accuracy in detection of hydrocarbon underneath seafloor.

REFERENCES

[1] http://www.epa.gov/esd/cmb/GeophysicsWebsite/pages/reference/methods/Marine_Geophysical_Methods/Marine_Seismic_Methods.htm

[2] Hanita Daud, Noorhana Yahya, Vijanth Asirvadam. "Development of EM Simulator For seabed logging application using MATLAB". Indian Journal od Geo-Marine Science

[3] EN Kong H. Westerdhal "Seabed Logging : A possible direct hydrocarbon for deepsea prospects using EM energy". Oslo : Oil & Gas Journal, 2002. – May 13, 2002 edition.

[4] L-J. Gelius, "Muti-component Processing of Sea Bed Logging Data" Department of Geoscience, University of Oslo, Norway, *PIERS ONLINE*, Vol 2, No 6, 2006

[5] Anuar Bhuiyan, Tor wicklund, Stale Johansen, "High Resistivity Anomalities at Modgunn Arch in the Norwegian Sea", Technical Article, first break volume 24, January 2006.

[6] http://www.lbl.gov/cs/Archive/news093009.html

[7] S. E. Johnstad, H. Westerdahl, F. N. Kong, and Z. Wang, "Comparison of Antenna Types and Orientations for Detecting Hydrocarbon Layers in Seabed Logging"

[8] S. E. Johnstad, B. A. Farrelly, Hydro O&E and C. Ringstad, "Seabed logging on the North Sea Troll Field", Offshore Technology Conference, 2 – 5 May 2005.

[9] http://www.ogj.com/articles/print/volume-100/issue-19/special-report/seabed-logging-a-possible-direct-hydrocarbon-indicator-for-deepsea-prospects-using-em-energy.html

[10] Johansen, S. E., Amundsen, H. E. F., Rosten, Ellingsrud, S., Eidesmo, T., Bhuyian, A. H., (2005). Subsurface Hydrocarbons Detected by Electromagnetic Sounding. *First break*, 23, 31-36.

[11] STATOIL ASA, 2005, Electromagnetic Data Processing, WO 2005/096019 A1, Patent Cooperation Treaty (PCT).

[12] The Oilfield Glossary- Forward Modeling (n.d). Retrieved March 17, 2010 Retrieved from http://www.glossary.oilfield.slb.com/Display.cfm?Term=forward%20modeling

[13] Gelius, L., (2006). Multi-component Processing of Sea Bed Logging Data. *PIERS ONLINE.* 2(6), 589 – 593. doi: 10.2529/PIERS060822070325

[14] Fawwaz T.Ulaby, Magnetostatics, Electromagnetics for Engineers, Pearson Education International, The University of Michigan, (2005)

[15] http://www.ainc-inac.gc.ca/ai/scr/nt/ntr/pubs/og-eng.asp

[16] http://www.lbl.gov/cs/Archive/news093009.html

[17] http://www.sciencedirect.com/

[18] Scandinavian Oil & Gas Magazine The Rapid Adoption of Seabed Logging [Magazine]. - Artic Alaska: Oil & Gas, 2007 – No. 5/6

[19] Janniche Iren Nordskag and Lasse Amundsen, "Asymptotic airwave modeling for marine controlled-source electromagnetic surveying", Society of Exploration Geophysicsts

[20] L.O Loseth, L. Amundsen, " On the Signal Proapagation in Marine CSEM" , EGM 2007 International Workshop, Innovation in EM, Grav, Mag Methods, a new Prospective for Exploration, Capri, Italy, 15-18 April 2007

[21] Jones, Childers, " Contemporary College Physic " , 3_{rd} Edition, McGraw-Hill, 530, dc-21

[22] D. Ridyard (2008). Seabed Logging – A proven Tool for Offshore Exploration and Development. Retrieved July 13, 2010, From http://www.searchanddiscovery.net/documents/2008/08008ridyard/index.htm.